

1 HSPB2 Facilitates Neural Regeneration for Sensorimotor Recovery after
2 Traumatic Brain Injury through Autophagy

3 Yichen Huang¹, Shan Meng¹, Biwu Wu², Hong Shi³, Yana Wang¹, Jiakun Xiang¹, Jiaying Li¹, Ziyu Shi
4¹, Gang Wu², Yanchen Lyu¹, Xu Jia¹, Jin Hu², * Zhi-Xiang Xu¹ and * Yanqin Gao¹

5¹ State Key Laboratory of Medical Neurobiology, MOE Frontiers Center for Brain Science, and Institutes of
6 Brain Science, Fudan University, Shanghai, China;

7² Department of Neurosurgery, Huashan hospital, Fudan University, Shanghai, China

8³ Department of Anesthesiology, Shanghai Pulmonary Hospital, School of Medicine, Tongji University,
9 Shanghai, China;

10 *Corresponding Author

11 Yanqin Gao

12 State Key Laboratory of Medical Neurobiology, Fudan University, Shanghai 200032, China.

13 **Email:** yqgao@shmu.edu.cn, Telephone: +8621 54237778

14 Zhi-Xiang Xu

15 MOE Frontiers Center for Brain Science, and Institutes of Brain Science, Fudan University, Shanghai 200032,
16 China.

17 **Email:** zhixiangxu@fudan.edu.cn

18

19 **This PDF file includes:**

20

21 Supplemental Methods

22 Figure S1 to S11

23 Table S2

24 Legends for Movies S1 to S2

25 Supplemental References

26

27 **Other supporting materials for this manuscript include the following:**

28	Tables S1, 3, 4
29	Movies S1 to S2
30	Supporting data
31	

32 Supplemental Methods

33 *Animals.*

34 C57BL/6J mice were purchased from Shanghai Jie Si Jie Laboratory Animal Co., Ltd. HSPB2 knock-in mice
35 (C57BL/6-*Gt (ROSA)26Sor^{em1} (CAG-LoxP-STOP-LoxP-HSPB2-3×HA-WPRE-polyA)*, *Hspb2* gene ID: CCDS8352, abbreviated
36 as *R26-e(CAG-LSL-Hspb2)*) were made from Shanghai Biomodel Organism Science & Technology
37 Development Co., Ltd., and *Map2-Cre^{ERT2}* mice (C57BL/6-*Map2^{em1(2A-CreERT2)Smoc}*, Cat# NM-KI-00037) were
38 also purchased from Shanghai Biomodel Organism. Neuron-specific HSPB2 overexpression [abbreviated as
39 TG (transgenic)] mice were obtained by crossing the *R26-e(CAG-LSL-Hspb2)* mice and *Map2-Cre^{ERT2}* mice
40 for two generations. The TG mice (genotype: *Rosa26^{LSL/LSL} × Map2^{CreERT2/wt}*) were viable, fertile, and normal
41 in size, displaying no apparent physical or behavioral abnormalities. To induce gene overexpression, TG
42 mice received intraperitoneal injections of tamoxifen (75 mg/kg daily for 5 days). Hemizygous *R26-e(CAG-*
43 *LSL-Hspb2)* mice (genotype: *Rosa26^{LSL/LSL} × Map2^{wt/wt}*) served as age- and sex-matched wild-type (WT)
44 control mice and received the same tamoxifen treatments. Mice were subjected to cortical controlled impact
45 10 days after tamoxifen treatments. For delayed tamoxifen induction, tamoxifen was administrated 7 days
46 post-impact for 5 days.

47 Male 9-12 weeks old (25~28g) or female 12-15 weeks (25g~28g) mice were used for the experiment. Mice
48 were housed in a pathogen-free facility with regulated temperature and humidity and a 12-h light/dark cycle.
49 Food and water were provided ad libitum. All animal experiments in the study were approved by the Animal
50 Care and Use Committee of Shanghai Medical College, Fudan University.

51

52 **Patients**

53 Brain tissues were collected from the damaged regions surgically removed from three patients with cerebral
54 contusion and laceration (Table 1) who underwent emergency neurosurgery operations in Huashan Hospital,
55 Shanghai, China. These tissues were marginal and inevitably excised during surgical removal of hematoma
56 and necrotic tissue, with all precautions taken to minimize damage to healthy tissue. Informed consent was
57 obtained from each patient and family. All patients had severe cerebral contusion and laceration, with no
58 prior history of brain injury or other neurological disorders. Upon removal, the tissue was quickly dehydrated
59 and paraffin-embedded, and sectioned into 10 μm slices for subsequent immunostaining.

60 **Table 1. Detailed information of patients**

Patients	Age	Gender	diagnosis	Tissue location	Tissue size (cm)	Admission neurological outcomes (GCS)
1	48	Male	Cerebral contusion and laceration	Left basal ganglia	2*1.5*0.6	10
2	54	Female	Cerebral contusion and laceration	Left basal ganglia	Diameter 1.5	3
3	32	Male	Cerebral contusion and laceration	Right basal ganglia	Diameter 0.3	14

61 GCS: Glasgow Coma Scale.

62

63 **TBI model**

64 TBI was induced using a cortical controlled impact (CCI) device (TBI 0310, Precision Systems and
 65 Instrumentation) following a previously described procedure(1). In brief, mice were anesthetized with 3 %
 66 isoflurane in a 70% N₂/30% O₂ mixture and fixed on stereotaxic apparatus maintaining breathing by animal
 67 respirator with 1.5 % isoflurane in 70% N₂/30% O₂ mixture and temperature by warming light. After
 68 sterilizing and removing hair, a midline incision was made to expose the skull. An approximate 4-mm
 69 craniotomy was performed over the right parietotemporal cortex using a motorized drill. The CCI was
 70 centered 2.5 mm lateral to the midline and 0.5 mm anterior to the bregma, conducted with a 3-mm flat-tip
 71 impounder. The CCI indexes were set as follows: velocity, 3.5m/s; duration, 150ms; depth, 1.5mm. After the
 72 CCI, the scalp incision was carefully sutured, and the mice were placed on a heating pad until recovery from
 73 anesthesia. Sham mice underwent all procedures except for CCI.

74

75 **Primary neuronal culture and oxygen/glucose deprivation (OGD)**

76 Cortical neurons were cultured from E16-18 fetal mice. The isolated cortex was removed and digested with
 77 20 U/ml papain in Dulbecco's modified eagle medium (DMEM) /F12 (Cat# 11320033, Gibco) at 37 °C for
 78 10 min. Dissociated neurons were cultured in Neurobasal media A (Cat# 21103049, Gibco) supplemented
 79 with 2% B-27 (Cat# 17504044, Gibco), 1% GlutaMAX (Cat# 35050079, Gibco), and 1% penicillin-

80 streptomycin (Cat# 15140163, Gibco) at 37 °C and 5% CO₂ incubator. On day 7, neurons were treated with
81 oxygen and glucose deprivation (OGD). In brief, the medium was replaced by glucose-free DMEM/F12
82 (Cat# 21331020, Gibco), and the culture was transferred to a chamber containing 5% CO₂, 90% N₂, and 5%
83 H₂ at 37 °C for 1 hour. Subsequently, the medium was replaced with normal neuron medium and the culture
84 was returned to 37 °C and 5% CO₂ incubator.

85 To achieve HSPB2 overexpression, primary neurons were cultured from TG (genotype: Rosa26^{LSL/LSL} ×
86 MAP2-Cre^{ERT2/wt}) fetal mice, and 4-hydroxytamoxifen (4-OHT, A56098, Beijing Wokai Biotechnology Co.,
87 Ltd) was added to the medium at the concentration of 2 μM on day 5 followed by subsequent OGD/r operation
88 on day 7.

89

90 **RNA silencing of Bag3**

91 Lentivirus vectors (pLentai-hU6-shRNA-esEF1A-MataGFP-WPRE-pA) containing shRNA targeting Bag3
92 (5'-AGGTCTCCTCTGCTCCAATTC-3', brief as shBAG3) and scrambled shRNA sequence were obtained
93 from Shanghai Taitool Bioscience Co.,Ltd. The scrambled shRNA sequence was used as a control (brief as
94 shSCR). To achieve BAG3 knockdown, the neurons were infected with lentivirus on day 4 by the MOI
95 (multiplicity of infection) = 1 for 24 h, then the virus-containing medium was replaced by normal neurobasal
96 medium.

97

98 **Immunofluorescence (IF) staining and data analysis**

99 Mice were deeply anesthetized with 1% pentobarbital sodium (50ml/kg) intraperitoneally before being
100 perfused intracardially with ice-cold saline and 4% paraformaldehyde. The brain was harvested and
101 cryoprotected sequentially in 4% paraformaldehyde, 20% sucrose in PB, and 30% sucrose in PB to complete
102 post-fixation and dehydration. 25μm coronal section was obtained using a freezing microtome (HM525NX,
103 Thermo Scientific).

104 Brain sections were washed with PBS and PBS+0.3% Triton, incubated in PBS+1% Triton X-100 to
105 permeabilize and blocked with 10% goat or donkey serum for 1h. M.O.M. Kit (Cat# BMK-2202, Vector
106 Laboratories) was used to block mouse antibodies. Brain sections were then incubated with primary
107 antibodies overnight at 4°C. After washing, the sections were incubated with secondary antibodies conjugated

108 with Alexa Fluor-405/488/594/647 (1:1000, Jackson ImmunoResearch Laboratories) for 2 hours at room
109 temperature. Slides were mounted with DAPI-Fluoromount-G (Cat# 0100-20, Southern Biotech).
110 Fluorescence images were captured using a Nikon A1 confocal microscope equipped with NIS-Elements
111 software (Nikon) or with Nikon ECLIPSE Ni-E microscope. Images were processed and analyzed with
112 ImageJ software (Fiji, NIH, <https://imagej.net/software/fiji/#publication>), and Z-series images were
113 processed and 3D-rendered with Imaris version9.0.1 (Oxford Instruments), as previously described (2).

114 To assess tissue loss, 10 serial sections with an interval of 11 sections were NeuN immunostained to calculate
115 the NeuN-immunopositive area (mm²) or volume (mm³) of tissue loss using ImageJ [area of tissue loss % =
116 (area of contralateral hemisphere - area of the ipsilateral hemisphere) / area of the ipsilateral hemisphere; the
117 volume of tissue loss % = $\sum (\text{area of tissue loss}) \times 25\mu\text{m} \times 12 / \sum \text{area of the ipsilateral hemisphere} \times 25\mu\text{m} \times$
118 12].

119 For biotinylated dextran (BDA) staining, a streptavidin blocking kit (SP-2002, Vector Laboratories) was used,
120 followed by immunostaining with streptavidin Alexa Fluor 488/647 (Invitrogen).

121 Cell counting was performed unbiasedly using ImageJ function Analyze Particles according to consistent
122 parameters, as previously described (2). In brief, positively stained cells were counted from two to three 40x
123 microscopic fields (317.4 $\mu\text{m} \times 317.4 \mu\text{m}$) in the cortex or striatum. A suitable threshold was established to
124 differentiate target signal from background using the Analyze Particles function. The process for β -amyloid
125 precursor protein (β -APP) quantification was consistent with cell counting. For $A\beta$ quantification,
126 fluorescence intensities were measured using ImageJ software by applying threshold adjustment, as described
127 previously (3).

128

129 **Immunoblotting (Western blotting)**

130 After perfusion, cortical tissue from the peri-injury region (about 4×4×2 mm) of both ipsilateral and
131 contralateral hemispheres was harvested, then homogenized and ultrasonicated with RIPA cell lysis buffer
132 (Cat# 9806, Cell Signaling Technology, Boston, USA), 1 mM PMSF, and phosphatase inhibitor cocktail
133 PhosSTOP (Cat# 4906845001, Roche, Basel, Switzerland) to extract proteins. Western blots were performed
134 using the standard SDS-polyacrylamide gel electrophoresis (PAGE) method. In brief, polyvinylidene
135 difluoride (PVDF) membranes were blocked with 5% nonfat milk for 1 h at room temperature and then

136 incubated overnight at 4 °C with primary antibodies. The membrane was then incubated with secondary
137 antibodies for 1 h at room temperature (1:10,000, Proteintech, Rosemont, IL, USA) and scanned using the
138 Bio-rad ChemiDoc system (Bio-rad, Hercules, CA, USA). ImageJ software was used for gel analyses.

139

140 **Real-time qPCR**

141 Total RNA was extracted from cortical tissue of the peri-injury region (about 4×4×2 mm) in the ipsilateral
142 hemisphere using TRIzol reagent (Invitrogen, Cat# 15596026). First-stand cDNA was generated using the
143 RevertAid First Strand cDNA Synthesis Kit (Thermo Scientific, Cat# K1622) according to the manufacturers'
144 protocols. The following primers were used for mouse samples:

145 *Hspb1*: Forward: ATCCCCTGAGGGCACACTTA-3'

146 Reverse: 5'-GGAATGGTGATCTCCGCTGAC-3'

147 *Hspb2*: Forward: 5'-CTCTATCCCATGATGGCATCCT-3'

148 Reverse: 5'-CTCAACTCTGGCTATCTCTTCCT-3'

149 *Hspb3*: Forward: 5'-GACCCCAGTGC GTTATCAGG-3'

150 Reverse: 5'-GGCTTTACTCAGGTCCTCGAT-3'

151 *Hspb5*: Forward: 5'-GTTCTTCGGAGAGCACCTGTT-3'

152 Reverse: 5'-GAGAGTCCGGTGCAATCCAG-3'

153 *Gapdh* : Forward: 5'-CTGCCAGAACATCATCCCT-3'

154 Reverse: 5'-TGAAGTCGCAGGAGACAACC-3'

155 Real-time qPCR was performed using SYBR Green Master Mix (Yeasen, Cat# 11201ES03) on
156 QuantStudio 5 (Thermo Scientific, Cat# A28140). All reactions were performed in triplicates, and the relative
157 amount of mRNA was normalized to GAPDH level.

158

159 **Behavior tests**

160 Behavioral tests were performed in a blinded manner and analyzed unbiasedly. Sensorimotor functions were
161 measured 3–35 d post-TBI. All behavioral testing was conducted during the light cycle phase. Mice were
162 trained for 3 days before surgeries to reach a close baseline.

163 The body curl test was used for detecting unilateral lesions(4). Mice were hand-suspended by the tail and
164 rated for degree of torso flexion from vertical towards the contralateral injury side. The degree of body curl
165 was rated as absent (1), mild (2), moderate (3), and severe (4). Normal mice hang vertically without flexion
166 and thus deviate 0° from vertical (rating of 1). Flexion of the torso at 22.5° from vertical was rated 2 (mild);
167 flexion between 22.5° and 45° from vertical was rated 3 (moderate), and flexion of the torso at 45° or more
168 and with/or without grasping of the hindlimbs by forelimbs was given a rating of 4 (severe).

169 The foot fault test (grid-walking test) was performed as described previously(5) to assess sensorimotor
170 coordination. Mice were placed on an elevated grid surface (30 cm (L) × 35 cm (W) × 31 cm (H)) with a grid
171 opening of 2.25 cm² (1.5 cm × 1.5 cm square) and videotaped for 3 min from below the grid. The videotapes
172 were analyzed by a blinded investigator to count the number of total steps and the number of foot faults made
173 by the impaired limbs. Foot faults were determined when the mouse misplaced its left forepaw such that the
174 paw fell through the grid, and expressed as a percentage of total steps. The foot-fault rate = the number of
175 foot faults / the number of total steps.

176 The rotarod test was performed by a rotating drum (Ugo Basile, Gemonio, Italy). Briefly, mice were forced
177 to run on the rotating drum with speeds starting at 4 rpm and accelerating to 40 rpm within 300 s. Three
178 consecutive trials were conducted for each mouse with an interval of 15 min. The time at which a mouse fell
179 off the drum was recorded as the latency to fall. Data were expressed as mean values from three trials.

180 The Morris water maze test was carried out 29-34 days following TBI to evaluate spatial cognitive functions
181 as described previously(6). Briefly, in the learning stage (day 29-33), a square platform (11 × 11 cm²) was
182 submerged 2 cm beneath the water surface in a circular pool (diameter = 109 cm) filled with opaque water.
183 Mice were placed into the pool at one of the four locations and given 60 seconds to locate the hidden platform.
184 At the end of each trial, the mouse was placed on the platform or allowed to stay on the platform for 30 s
185 with prominent spatial cues displayed around the room. The time spent to reach the platform (learning phase)
186 was recorded. Four trials were performed each day with randomly assigned orders. The memory test was
187 performed on day 34. The platform was removed, and a single 60-s probe trial was conducted. Time spent in
188 the target quadrant where the platform was previously located was recorded.

189

190 **MRI**

191 For in vivo MRI, mice were initially anesthetized with 3% isoflurane and positioned on an animal cradle with
192 a stereotaxic head holder. Anesthesia was maintained between 1% and 1.5% isoflurane throughout the
193 experiment. Respiration and temperature were monitored continuously. MRI was performed with an 11.7T
194 small animal system (Bruker BioSpec 117/16) with a 6-mm 4-channel surface array coil (Bruker BioSpin,
195 Billerica, MA). The DTI data were collected using a spin echo imaging (SE)- DTI imaging sequence using
196 the following setup: TR/TE = 50,00/24 ms, Direction = 30, FOV = 20 ×20 mm, acquisition matrix = 200 ×
197 200, 30 slices with a slice thickness of 0.5 mm, 3 averages, 4 segments, and a b-value = 1,000 s/mm².
198 Perfusion-fixed brains at day 49 were left in the skull and imaged ex vivo using the following setup: a SE
199 sequence with 60 directions, TR/TE = 80/19 ms, FOV = 16 ×16 mm, acquisition matrix = 80 × 80, 74 slices
200 with a slice thickness of 0.2 mm, 3 averages, 4 segments, and a b-value = 2,000 s/mm². DTI data were
201 analyzed with DSI Studio software (<http://dsi-studio.labsolver.org/>). ROIs were drawn manually in a blinded
202 manner encompassing the EC (external capsule) and STR (striatum) in the ipsilateral and contralateral
203 hemispheres to determine FA and RD. DEC, FA, and RD maps were generated by DSI Studio software.
204 Tracks across the midline of CC (corpus callosum) were traced and quantified by DSI Studio.

205

206 **Electrophysiology**

207 Compound action potentials (CAPs) in the external capsule were recorded as previously described(7). Mice
208 were anesthetized with isoflurane and were decapitated to remove the brains rapidly. A 350- μ m coronal brain
209 slice was prepared using a vibratome (1200s, Leica). Slices were transferred to artificial cerebrospinal fluid
210 (aCSF) saturated with 95% O₂+5% CO₂ mixture at 32°C for 0.5 h then at room temperature for 1 h for
211 recovery. The aCSF contained 124 mM NaCl, 2.5 mM KCl, 2 mM CaCl₂, 1 mM NaH₂PO₄, 24 mM NaHCO₃,
212 1.3 mM MgSO₄, and 10 mM D-glucose. A concentric stimulating electrode and a glass microelectrode (5~8
213 M Ω) were used for stimulating and recording. CAPs were induced by monophasic square waves (0.1 ms
214 duration) with a stimulus generator (STG 4002, Multichannel). Evoked signals were amplified by Axoclamp
215 700B (Molecular Devices) and digitized Axon Digidata 1440A (Molecular Devices).

216

217 **BDA tracing**

218 Biotinylated dextran amine (BDA, 10,000 MW, Invitrogen, Cat# D1956) was intracerebrally injected to
219 anterograde trace the projection of motor neurons, and label corticospinal tract (CST). Briefly, 2 μ l of BDA
220 (10% wt/vol, dissolved in PBS) was stereotactically injected into contralateral cortex (bregma: AP = 0.6 mm,
221 ML = 1.2 mm, and DV = 1.5 mm, M1 zone). After 14 days, mice were sacrificed and coronal sections (25
222 μ m) of the cerebra, cerebellum, and spinal cord were collected. The numbers of BDA fibers across the midline
223 of cerebra corpus callosum (CC) layer (bregma 0mm), medulla oblongata facial nucleus (FN) layer (bregma
224 – 6.36mm), and spinal cord C7 layer were analyzed to assess physiological crossover and compensatory
225 sprouting. The labeled CST naturally crossed to the contralateral side at the corpus callosum in the cerebrum
226 (CC) and the pyramidal tract in the medulla oblongata facial nucleus layer (FN). Compensatory sprouting
227 occurred at the spine cord cervical layer 7 (C7) towards the injured limb.

228

229 **Calcium fiber photometry recording**

230 In vivo calcium fiber photometry recording was used to assess the cortical remapping of the ascending
231 sensory pathway. For the surgery, mice were anesthetized and the whole contralateral skull, bregma, and
232 lambda were exposed, avoiding exposure to the ipsilateral impact area. AAV2/9-hSyn-GCaMP6m-WPRE-
233 pA (Shanghai Taitool Bioscience, Shanghai, China, 10^{12} V.G./mL, 400 nL) was stereotactically injected into
234 the contralateral cortex [bregma: AP = 0.5 mm, ML = 2.0 mm, and DV = 1.7 mm, forelimb first sensory zone
235 (S1 FL)]. After injection, a ceramic optical fiber [1.7 mm length, O.D. = 160 μ m, numerical aperture (NA) =
236 0.37] was inserted into the injection area (bregma: AP = 0.5 mm, ML = 2.0 mm, and DV = 1.5 mm). Glue,
237 screw, and dental cement were used to secure the optical fiber, then mice were carefully placed on a warm
238 heating-pad until they woke up. Mice were individually housed and allowed to recover for at least two weeks.
239 For recording, the 3-color single-channel fluorescence recording system (Thinkertech, Jiangsu, China) was
240 used. The 470-nm channel was used for recording, while the 405-nm channel served as the control. The light
241 power was adjusted to 30 μ W to minimize bleaching. Then the optical fiber was attached to the recording
242 fiber linking to the system. During recording, mice remained awake, and a 100 Hz tactile stimulus was
243 applied to each side of the forepaw for 1 second by a modified device in turn (Video.S2). For each side of
244 the forepaw, 3 trails were recorded. Normalized $\Delta F/F$ was used to evaluate calcium activities. Analysis was

245 performed on the system's software and Matlab (Mathworks). The reference baseline time period is - 5~0 s,
246 when 0 is the time to deliver the tactile stimulus. The original $\Delta F/F$ was z-scored by each trial (both paws),
247 and the mean $\Delta F/F$ of 0~1 s was calculated to evaluate the calcium activity responding to stimulation.

248

249 **AAV-LC3 labeling**

250 AAV-mRFP-GFP-LC3 (pHBAAV-CMV-mCherry-EGFP-LC3) was bought from Hanbio (Shanghai, China)
251 and stereotactically injected into the ipsilateral and contralateral cortex (bregma: AP = -1 mm, ML = 2.0 mm,
252 and DV = 1.5 mm) of mouse (2 μ l) 14 days before TBI to label autophagic flux. Briefly, after perfusion and
253 dehydration, serial coronal sections (25 μ m) were collected and photographed. Z-series images were
254 processed and 3D-rendered using Imaris version 9.0.1 (Oxford Instruments). Since GFP degrades in an acidic
255 environment while RFP does not, yellow puncta (formed out of the overlap between red and green) indicate
256 autophagosomes, while red puncta indicate autolysosomes. About 5 cortical pyramidal neurons labeled were
257 labeled in each hemisphere and randomly selected for further analysis. Pyramidal neurons were identified
258 based on the morphology of long axons and dendrites by weak GFP fluorescence. For each hemisphere, 5
259 labeled pyramidal neurons were randomly chosen for further rendering and analysis.

260

261 **CQ application**

262 Chloroquine (CQ, Sigma, Cat# C6628, dissolved in saline solution at 6.25 mg/mL) was intraperitoneal
263 injected (0.625mg/g) 1 hour following TBI and daily till day 3 or 7 to block autophagic flux. Chloroquine
264 accumulates in acidic lysosomes, raising the lysosomal pH, thus inhibiting lysosomal hydrolases and
265 preventing autophagosome fusion and degradation.

266

267 **Immunoprecipitation**

268 After perfusion, cortex and hippocampus tissues or peri-injury area (about 4×4×2 mm) from the ipsilateral
269 hemisphere were harvested, homogenized, and ultrasonicated with Lysis Buffer for WB/IP Assays (Cat#
270 20118, Yeasen, Shanghai, China) and 1 mM PMSF to acquire undivided protein. SureBeads Protein G
271 Magnetic Beads (Cat# 1614021, Bio-Rad) were added to either anti-HA-Tag antibody (Mouse, #2367S, Cell
272 Signaling Technology, 1:200) or IgG for 10 minutes, and added to the cleared cell lysates. The mixture was

273 incubated at room temperature for 1 h. Immunoprecipitates were eluted with 20 mM glycine (pH 2.0) and
274 neutralized with 1 M phosphate buffer (pH 7.4). SDS-loading buffer was added and the mixture was heated
275 at 95 °C for 10 minutes for subsequent immunoblotting analysis.

276

277 **Immuno-co-localization analysis**

278 The co-localization of the target protein with another protein was assessed by plot profile and Spearman's
279 coefficient. For the plot profile, a line across the interested region was drawn and the ImageJ *plot profile*
280 function was used to visualize the distribution of the fluorescence intensity of the target protein and the other
281 protein along the same line. For Spearman's coefficient, ImageJ function *coloc 2* was used to assess the
282 colocalization of the target protein and the other protein in the same region of interest. About 10-15 neurons
283 were randomly selected for analysis.

284

285 **Docking prediction**

286 Protein structures were obtained from AlphaFold Protein Structure Database (<https://alphafold.com/>, HSPB2:
287 AF-Q16082-F1, APP: AF-P05067-F1, BAG3: AF-O95817-F1). Docking was predicted by GRAMM-X
288 (<http://gramm.compbio.ku.edu/>) with the rigid docking method. Interactions of the predicted docking
289 structure were quantified by PDBePISA(https://www.ebi.ac.uk/msd-srv/prot_int/cgi-bin/piserver). The
290 interface area and ΔiG were calculated to assess the stability of the docking structure. Protein structure and
291 intermolecular hydrogen bonds were visualized by Discovery Studio Version 4.5 (BIOVIA).

292

293 **Antibodies**

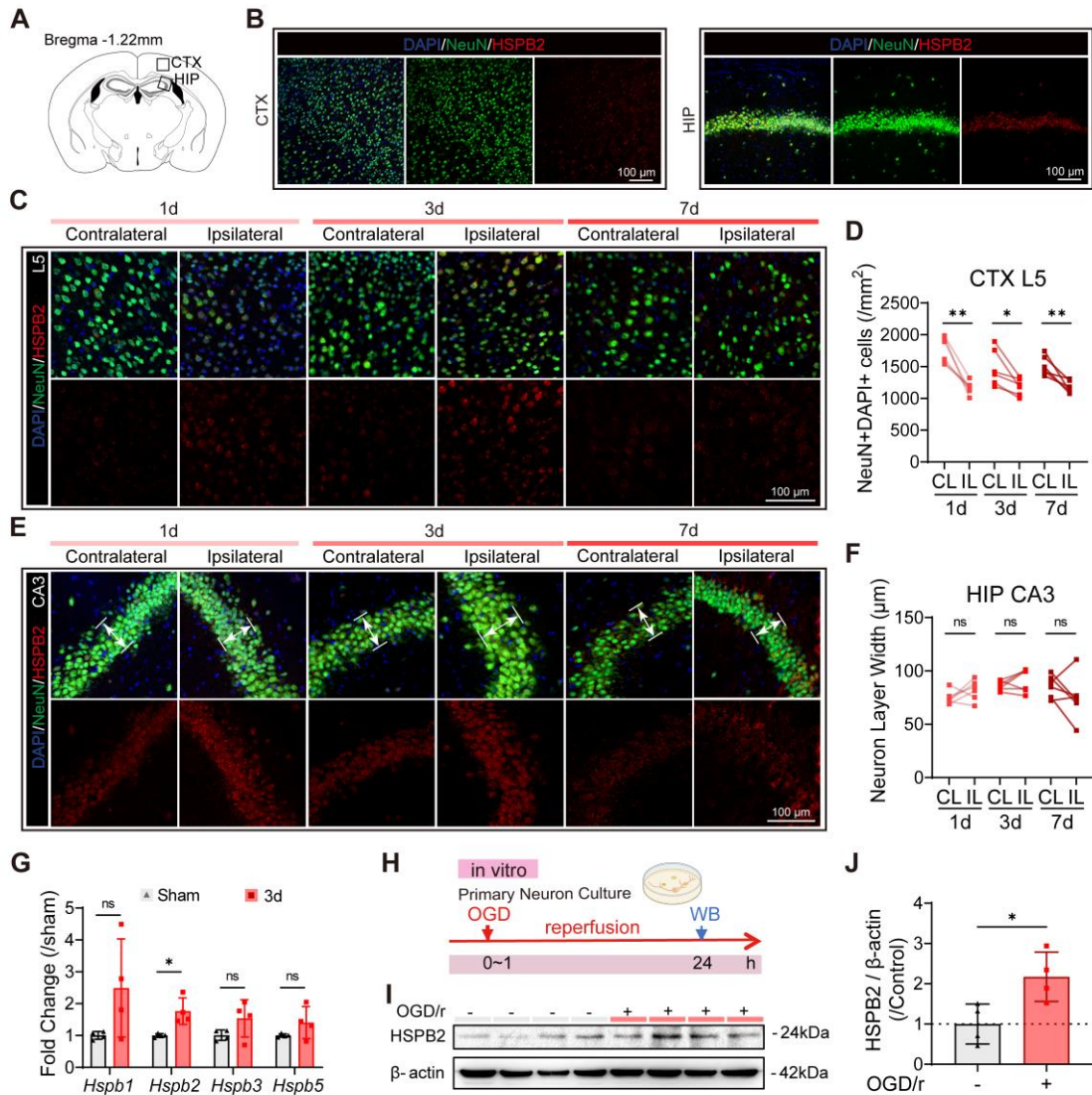
294 **Table 2. Antibody**

Antibody	Host	Company	Category	Dilution
NeuN-Alexa Fluor 488	Rb	Abcam	Ab190195	1:1000
NeuN	Rb	Abcam	Ab104225	1:1000
HSPB2	Rb	SAB	#38402	1:200
Iba1	Goat	Abcam	Ab5076	1:1000
GFAP	Ms	Invitrogen	14-9892-82	1:1000

β -actin	Ms	Proteintech	60008-1-Ig	1:10000
HA-Tag	Rb	CST	#3724	1:1000
HA-Tag	Ms	CST	#2307	1:1000
Synaptophysin	Rb	Abcam	ab32127	1:200
LC3	Rb	Proteintech	14600-1-AP	WB: 1:4000 IF: 1:400
SQSTM1	Rb	Proteintech	18420-1-AP	WB: 1:8000 IF: 1:200
Akt	Rb	CST	#4691	1:1000
beta Amyloid (CT695) (β APP)	Rb	Invitrogen	51-2700	1:1000
β -Tubulin (TUBB3) -Alexa Fluor 488	Rat	Abcam	ab195883	1:1000
BAG3	Rb	CST	# 23842	1:1000
Neurofilament heavy polypeptide (NF200)	Rb	Abcam	ab8135	1:1000
beta Amyloid (2C8) ($A\beta$)	Ms	Invitrogen	MA125493	1:1000
p-Akt (pS473)	Rb	Epitomics	2118-1	1:1000
mTOR	Rb	CST	#2983	1:1000
p-mTOR	Rb	CST	#5536	1:1000
GAP43	Rb	CST	#8945	1:1000

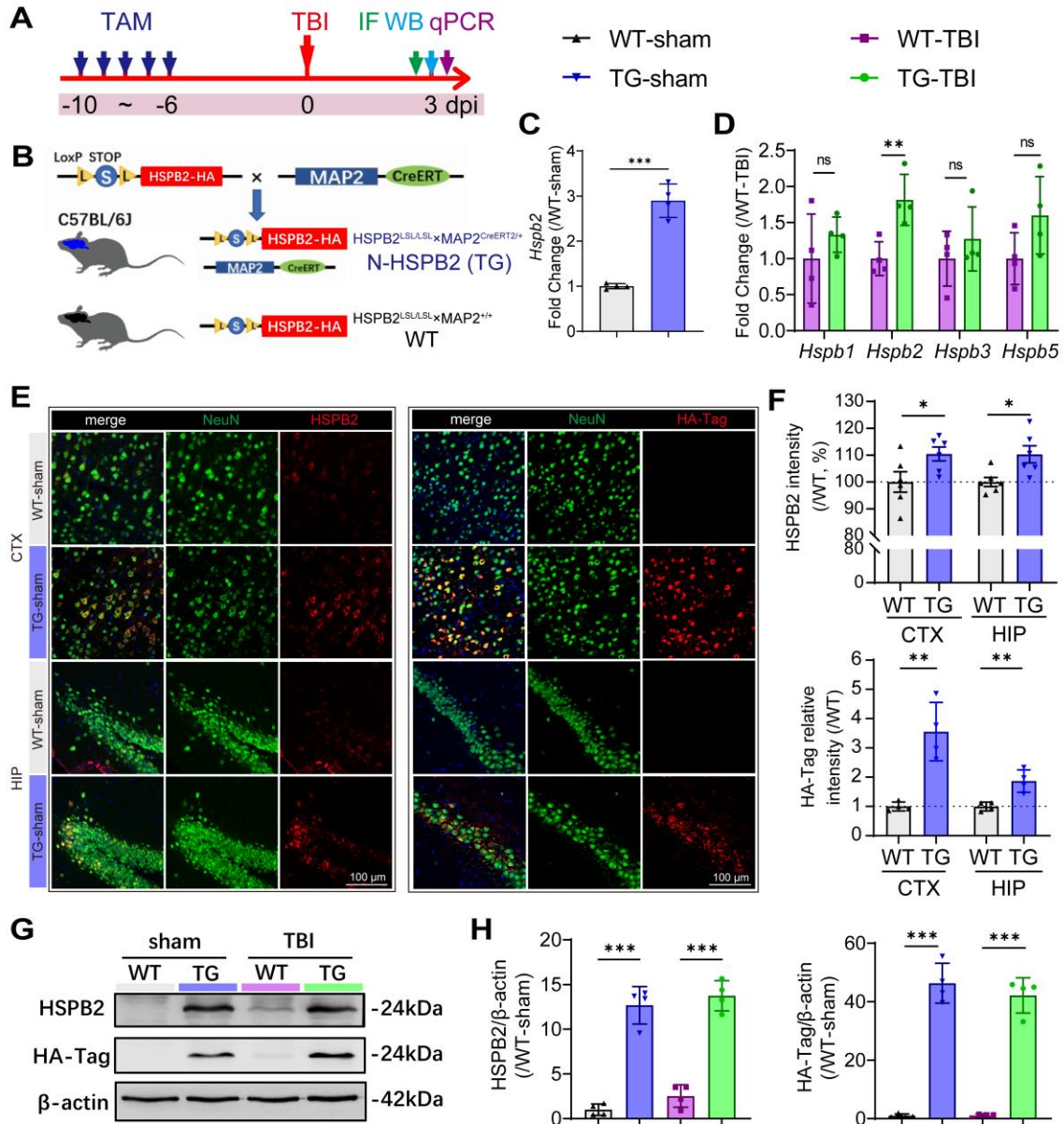
295

Rb: rabbit; Ms: mouse.



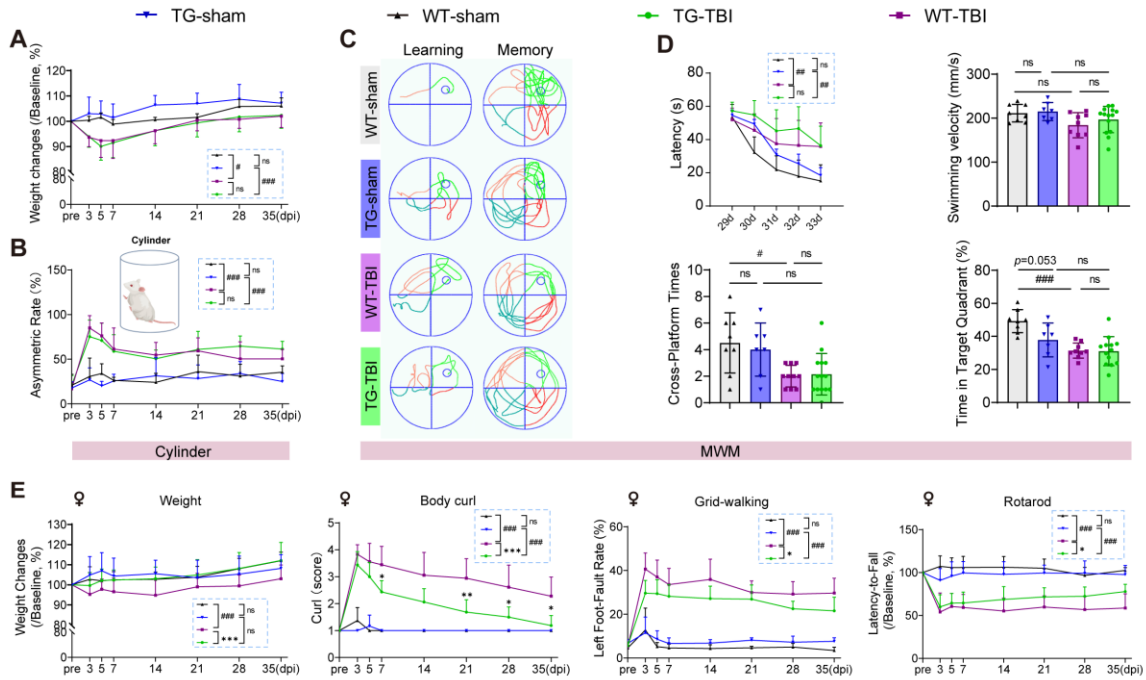
297

298 Figure S1 **Physiological and post-TBI HSPB2 expression in neurons.** A Region of interest (ROI) of cortex
 299 (CTX) and hippocampus (HIP) in the layer of post bregma 1.22mm; B Triple-label immunofluorescence of
 300 HSPB2(red)/NeuN(green, for neurons)/DAPI(blue) in CTX and HIP of normal brain, scale bar = 100 µm; C
 301 Representative images of HSPB2 expression in neurons at 1, 3, and 7 days in CTX Layer 5 (L5) after CCI,
 302 scale bar = 100 µm; D Quantitative analysis of neuron density in CTX neuron layer 5 at different time, n=6,
 303 analyzed using paired Student's t-test; E Representative images of HSPB2 expression in neurons at 1, 3, and
 304 7 days in HIP CA3 after CCI, arrowed line indicates neuron layer width, scale bar = 100 µm; F
 305 Quantitative analysis of CA3 neuron layer width at different time, n=6, analyzed using paired Student's t-test;
 306 Quantitative analysis of mRNA levels of *Hspb1*, 2, 3, and 5 at 3 days post TBI, n=4, analyzed using unpaired
 307 Student's t-test; H Experimental design of in vitro primary neuron culture OGD model; I&J Representative
 308 image of western blot and quantitative analysis of lysate HSPB2 relative expression after OGD/r in primary
 309 neuron culture, n=4, analyzed using unpaired Student's t-test. *: $p < 0.05$, **: $p < 0.01$, ns: no significance,
 310 as indicated.



311

312 Figure S2 **Verification of HSPB2 overexpression transgenic mice.** **A** Schematic diagram of the experiment, TAM: tamoxifen; **B** Construction of Tamoxifen-induced neuron-specific HSPB2 overexpression mouse ; **C**
 313 Quantitative analysis of the mRNA levels of *Hspb2* at 3 days after injury, n=4, analyzed using one-way ANOVA and post hoc Bonferroni test; **D** Quantitative analysis of the mRNA levels of *Hspb1*, 2, 3, and 5 at
 314 3 days post TBI, n=4, analyzed using unpaired Student's t-test; **E&F** Representative images and quantitative analysis of HSPB2 (E left & F up) and HA-Tag (E right & F down) expression in neurons in TG and WT
 315 (wild-type) mice, blue: DAPI, green: NeuN, red: HSPB2 or HA-Tag, scale bar = 100 μm, n=6, analyzed using unpaired Student's t-test; **G&H** Representative images and quantitative analysis of HSPB2 and HA-
 316 Tag relative expression at 3 days after injury, n=4, analyzed using one-way ANOVA and post hoc Bonferroni
 317 test. *: $p < 0.05$, **: $p < 0.01$, ***: $p < 0.001$, as indicated.
 318
 319
 320
 321
 322



323

324 **Figure S3 Improved behavioral tests of male and female following TBI in TG mice.** **A** Weight changes

325 following TBI, n=7, 7, 15, 17, respectively, analyzed using two-way ANOVA and post hoc Bonferroni test;

326 **B** The forelimb asymmetry rate in the cylinder test, n=7, 7, 15, 17, respectively, analyzed using two-way

327 ANOVA and post hoc Bonferroni test; **C** Representative routes of MWM during learning (d33) and memory

328 (d34) stages; **D** Quantitative analysis of MWM, including learning stage latency from d29 to d33 (upper left),

329 swimming velocity at d34 (upper right), platform crossing times at memory stage (lower left), and target

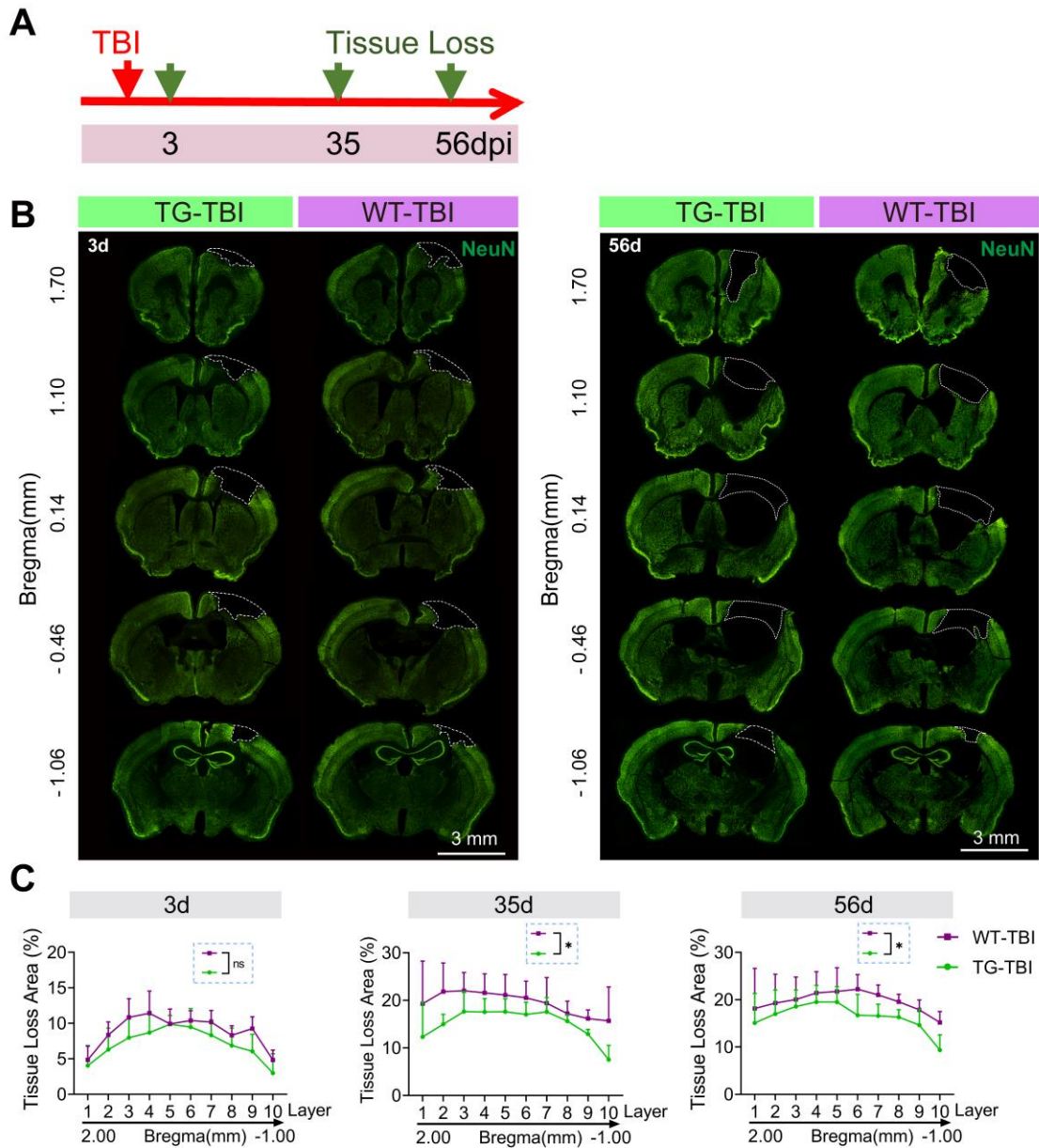
330 quadrant traveling time (lower right), n=7, 7, 10, 15, respectively, analyzed using two- and one-way ANOVA

331 and post hoc Bonferroni test; **E** Weight changes and behavioral tests for female mice, analyzed using two-

332 way ANOVA and post hoc Bonferroni test. * TG vs. WT, # TBI vs. sham; */#: $p < 0.05$, **: $p < 0.01$, ***/###:

333 $p < 0.001$, ns: no significance, as indicated.

334



335

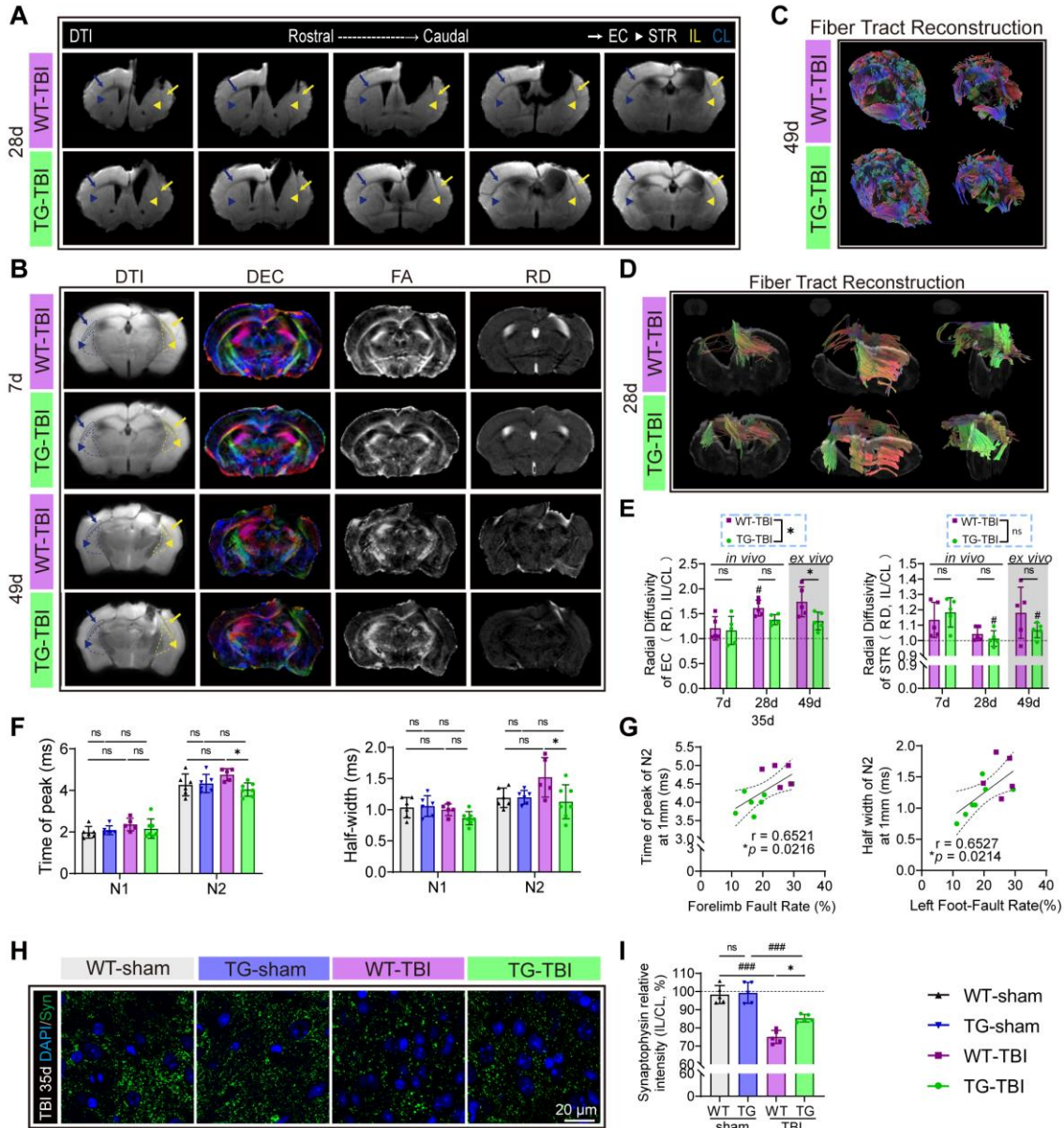
336 Figure S4 **Alleviated tissue loss following TBI in TG mice.** **A** Experimental design; **B** Illustration of tissue

337 loss in injured layers at 3 and 56 days post-injury, with dotted boxes indicating loss area, scale bar = 3 mm;

338 **C** Quantitative analysis of tissue loss area in injured layers, n=5-7, analyzed using two-way ANOVA and

339 post hoc Bonferroni test. *: $p < 0.05$, ns: no significance, as indicated.

340



342

343 Figure S5 Improved white matter integrity following TBI in TG mice verified by DTI and CAP. A

344 Illustration of DTI-MRI in different layers on day 28, triangle-arrowed dotted boxes indicate ROI STR,

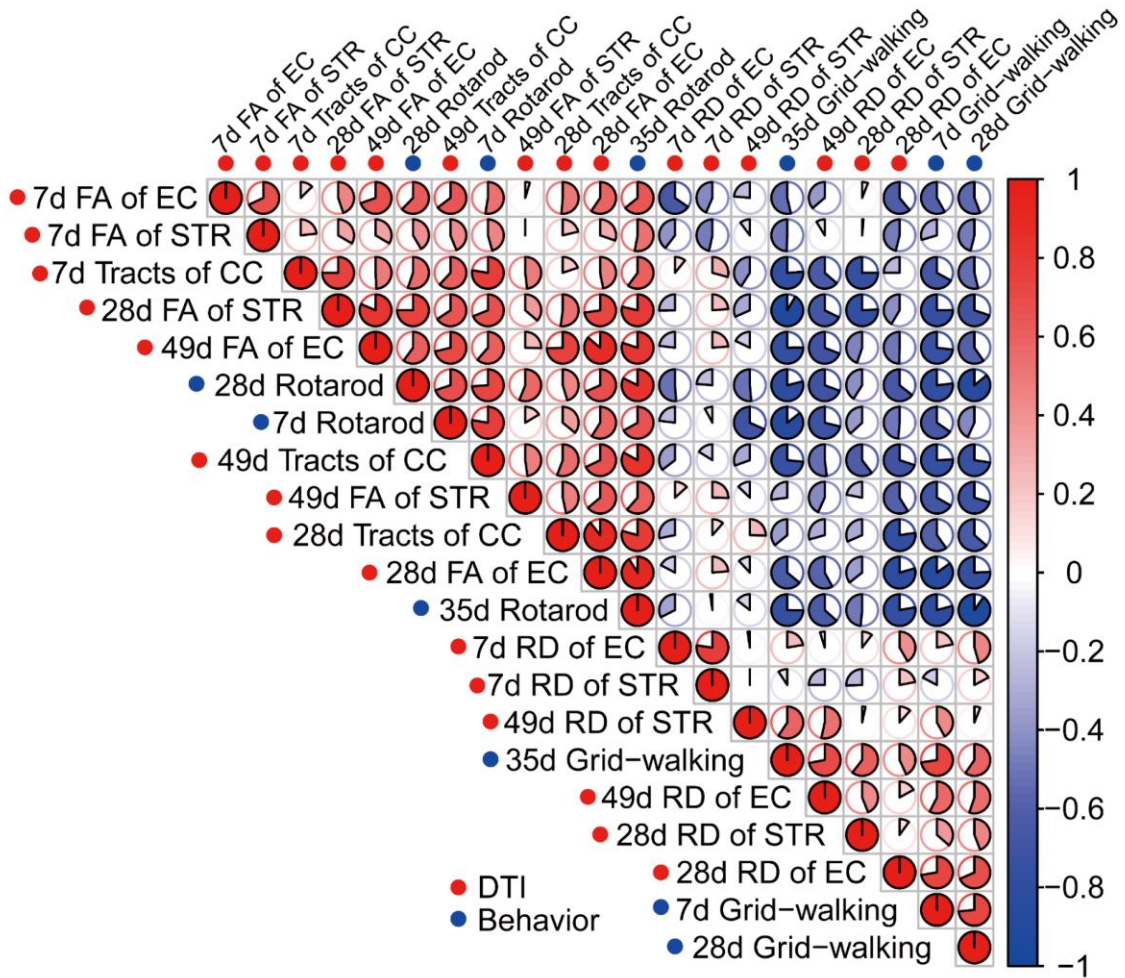
345 arrowed dotted boxes indicate ROI EC, yellow indicates the ipsilateral, blue indicates the contralateral; B

346 Illustration of DTI-MRI and visualized parameters on day 7 (in vivo) and 49 (ex vivo); C Illustration of 3D

347 reconstruction of fiber tracts on day 49 ex vivo, color indicating direction, from left to right: whole brain

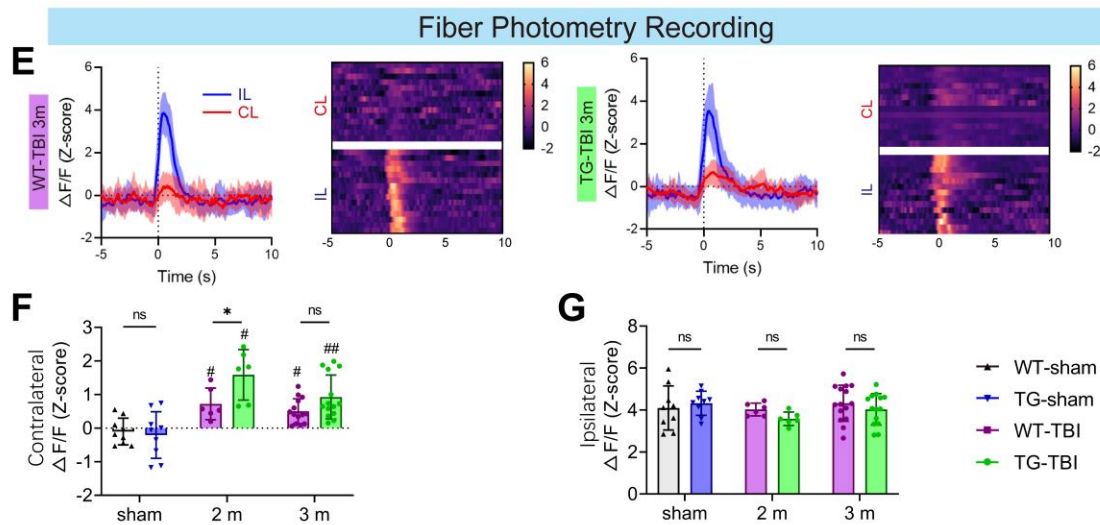
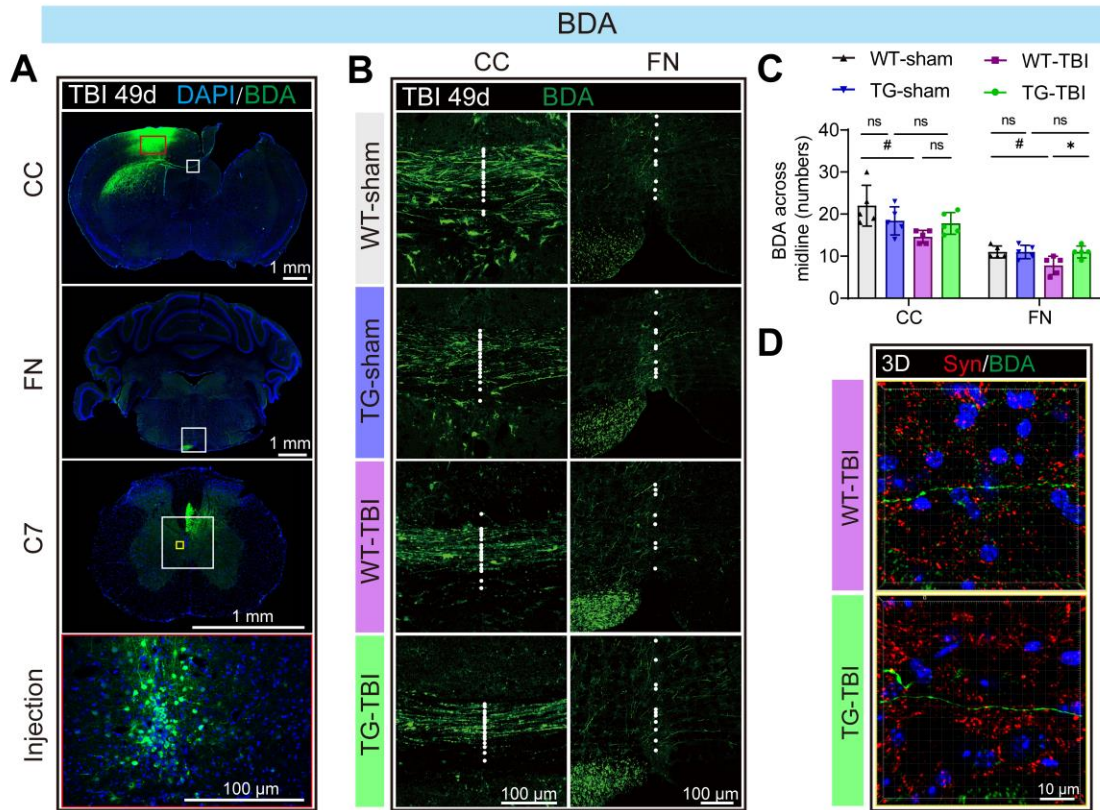
348 white matter fiber tracts, threshold-processed fiber tracts; D Illustration of 3D reconstruction of front view,

349 top view and side view of fiber tracts across the middle of CC on day 28 in vivo; **E** Quantitative analysis of
350 relative RD of EC and STR and fiber tracts across middle of CC normalized to WT-TBI at 7 and 28 days (in
351 vivo) and 49 days (ex vivo) following TBI, n=5, analyzed using two-way ANOVA and post hoc Bonferroni
352 test, * TG-TBI vs. WT-TBI, # indicates vs. 7d; **F** Quantitative analysis of time of peak and half-width of N1
353 and N2 of CAP, n=6-7, analyzed using one-way ANOVA and post hoc Bonferroni test. **G** Correlation
354 analysis of forelimb fault rate in grid-walking test with time of peak/half-width of N2 at 35 days post-injury,
355 r: Spearman correlation coefficient, n=6&7, analyzed using Spearman correlation test; **H** Illustration of
356 synapses around injured area at 35 days after injury, blue: DAPI, green: synaptophysin, scale bar = 20 μ m; **I**
357 Quantitative analysis of synapse density in h, n=5, analyzed using one-way ANOVA and post hoc Bonferroni
358 test. *: $p < 0.05$, ###: $p < 0.001$, ns: no significance, as indicated.
359



360

361 **Figure S6 Correlation matrix between DTI and behavior parameters.** Correlation matrix between DTI
 362 and behavioral indices at each time point, red: DTI indexes, blue: behavioral indexes, color intensity and fan
 363 size represent the Spearman r value, analyzed using Spearman correlation test.

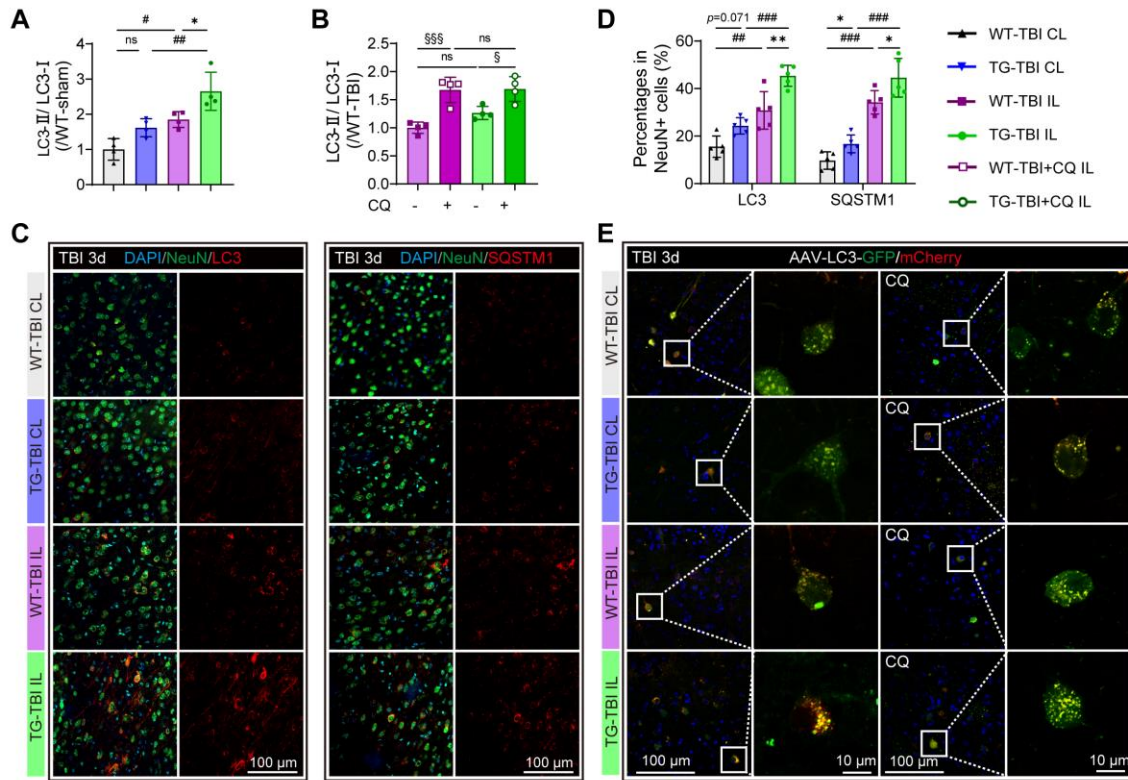


364

365 Figure S7 **Facilitated axon sprouting and cortical remapping following TBI in TG mice and verification**
 366 **of HPSB2 overexpression in vitro.** A Illustration of the BDA injection area and CST projection, CC:
 367 cerebrum corpus callosum layer, FN: medulla oblongata facial nucleus layer, C7: spine cord cervical segment
 368 7, red box indicates injection area, white box indicates ROI for BDA across the midline, and yellow box
 369 indicates ROI for synapses on newly-formed BDA⁺ axons, blue: DAPI, green: BDA, scale bar = 100 μ m &

370 1 mm; **B** Illustration of BDA labeled axons crossing the midline of CC and FN layer at 49 days after injury,
371 dot indicates the intersection of axon and midline, scale bar = 100 μm ; **C** Quantitative analysis of BDA⁺
372 axons crossing the midline of CC and FN layer at 49 days after injury, n = 5, analyzed using one-way ANOVA
373 and post hoc Bonferroni test; **D** Illustration of 3D images of synaptophysin vesicles in newly-formed BDA⁺
374 axons to be reconstructed in Figure 3F, blue: DAPI, red: synaptophysin, green: BDA, scale bar = 10 μm ; **E**
375 Line plots and heatmaps of the S1FL cortex fluorescent responses (z-scored $\Delta\text{F}/\text{F}$) from -5 to 10 seconds
376 after stimuli at each forepaw at 3 months, blue: ipsilateral, red: contralateral; **F&G** Quantitative analysis of
377 contralateral (f) and ipsilateral (g) forepaw $\Delta\text{F}/\text{F}$ from 2 to 3 months after injury, n = 3 \times 3 trails (sham), 2
378 \times 3 trails (2 months), 5 \times 3 trails (3 months) , analyzed using two-way ANOVA and post hoc Bonferroni test.
379 * TG vs. WT, # TBI vs. sham, */#: $p < 0.05$, **/##: $p < 0.01$, ***/###: $p < 0.001$, ns: no significance.

380



382

383 Figure S8 **Enhanced neuro-autophagy following TBI in TG mice. A&B** Quantitative analysis of LC3-II384 / I in Figure 4E, 4G, n=4, analyzed using one-way ANOVA and post hoc Bonferroni test; **C** Illustration of

385 LC3 (left) and SQSTM1 (right) levels in neurons in CTX 3 days following TBI, blue: DAPI, green: NeuN, red: LC3 (left) /

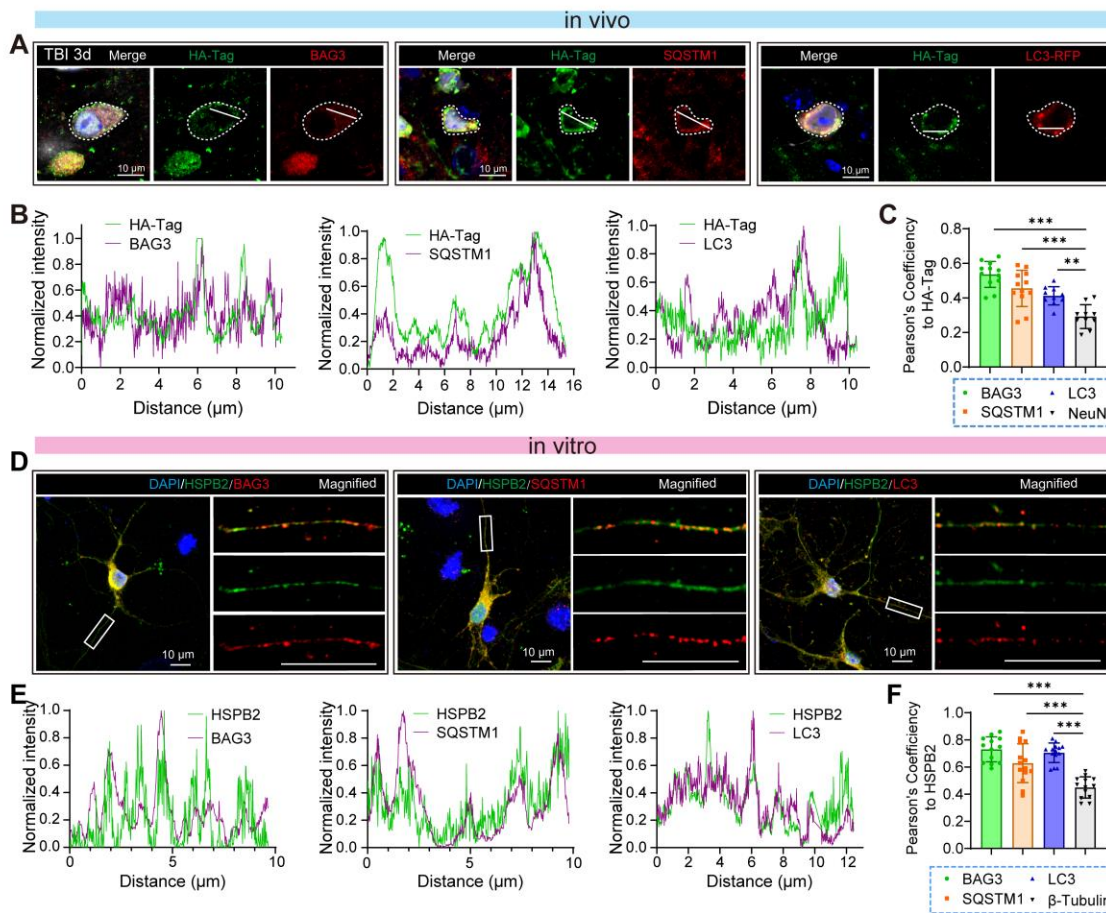
386 SQSTM1 (right), scale bar =100 μ m; **D** Quantitative analysis of LC3 and SQSTM1 positive neuron's percentages in total neurons in CTX 3 days following TBI n=5, analyzed using one-way ANOVA387 and post hoc Bonferroni test; **E** Illustration of autophagosome and autolysosome vesicles in neurons in CTX388 of ipsilateral and contralateral sides with/without CQ administration at 3 days following TBI, blue: DAPI, red: autolysosome, yellow: autophagosome, boxes indicate enlarged area. dpi: day post injury. *: $p < 0.05$,

389

390

391 **/###: $p < 0.01$, ###: $p < 0.001$, ns: no significance, as indicated.

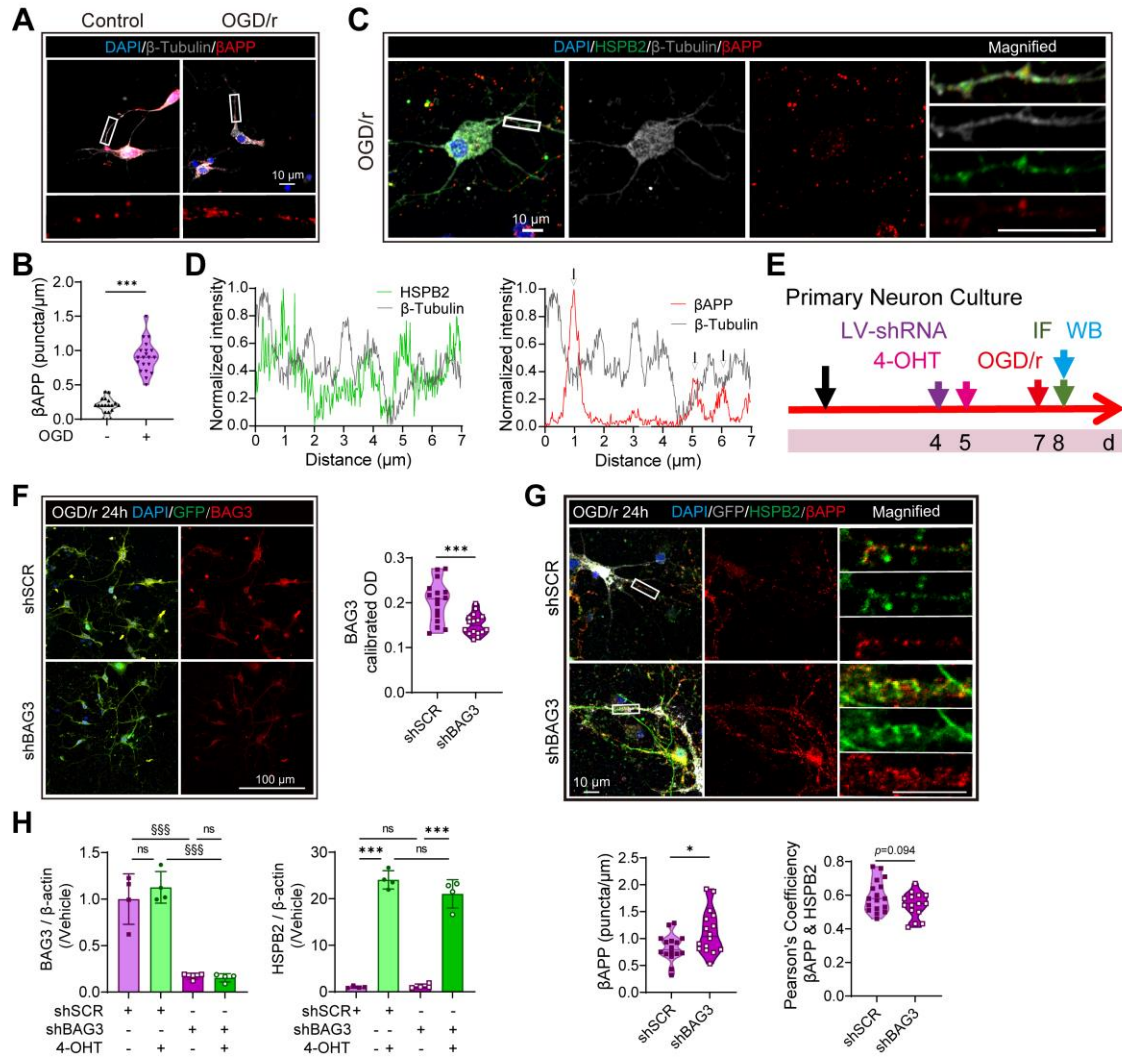
392



393

394 Figure S9 HSPB2's colocalization in vivo and in vitro. **A** Representative images of cell body colocalization
 395 of HA-Tag with BAG3, SQSTM1, and LC3 at 3 days following TBI, blue: DAPI, green: HA-Tag, red: BAG3,
 396 SQSTM1, and LC3, grey: NeuN, line indicates region of plot profile, scale bar = 10 μm ; **B** plot profile
 397 demonstrating cytosolic HA-Tag and BAG3/SQSTM1/LC3 colocalizations; **C** Quantitative analysis of
 398 Pearson's correlation coefficient of HA-Tag with BAG3, SQSTM1, LC3 and NeuN, n=10-15, analyzed using
 399 one-way ANOVA and post hoc Bonferroni test; **D** Illustration of axonal colocalization of HSPB2 with BAG3,
 400 SQSTM1, and LC3 in primary neuron culture after OGD, blue: DAPI, green: HSPB2, red: BAG3, SQSTM1,
 401 or LC3, box indicates magnified area, scale bar = 10 μm ; **E** plot profile demonstrating axonal HSPB2 and
 402 BAG3/SQSTM1/LC3 colocalizations; **F** Quantitative analysis of Pearson's correlation coefficient of HSPB2
 403 with BAG3, SQSTM1, LC3 and β -Tubulin, n=10-15, analyzed using one-way ANOVA and post hoc
 404 Bonferroni test. **: $p < 0.01$, ***: $p < 0.001$, ns: no significance, as indicated.

405



406

407

408 Figure S10 **β APP's presence in vitro and BAG3 silencing.** A&B Illustration and quantitative analysis of

409 axonal βAPP in primary neuron culture with or without OGD blue: DAPI, red: βAPP, grey: β-Tubulin, n =

410 20, analyzed using unpaired Student's t-test; C Illustration of axonal colocalization of βAPP with HSPB2

411 and β-Tubulin in primary neuron culture in OGD, blue: DAPI, green: HSPB2, red: βAPP, grey: β-Tubulin,

412 box indicates magnified area, scale bar = 10 μm; D Plot profile demonstrating axonal β-Tubulin and

413 HSPB2/βAPP colocalizations; E Experimental design for HSPB2 overexpression and BAG3 silence

414 experiments in vitro; F Illustration and quantitative analysis of BAG3 in primary neuron culture with shSCR

415 or shBAG3, blue: DAPI, red: BAG3, green: GFP, n = 16, analyzed using unpaired Student's t-test; G

416 Illustration and quantitative analysis of of axonal βAPP and its colocalization with HSPB2 in primary neuron

417 culture after OGD with or without BAG3 silencing, box indicates magnified area, scale bar = 10 μm, n=15-

418 17, analyzed using unpaired Student's t-test; G Quantitative analysis of BAG3 and HSPB2 24h post OGD

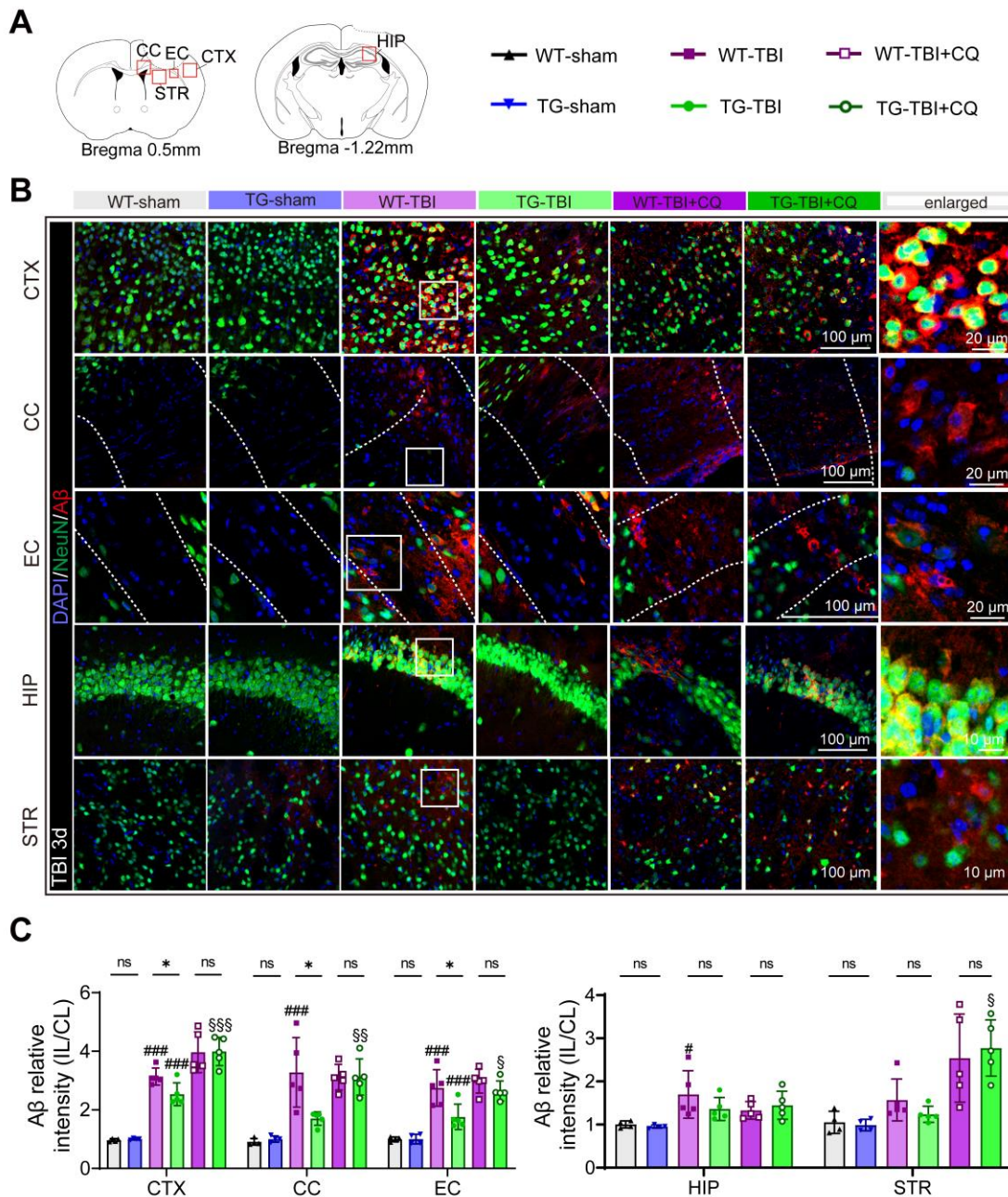
419 with or without BAG3 silencing or HSPB2 overexpression, n=4, analyzed using one-way ANOVA and post

420 hoc Bonferroni test. 4-OHT: 4-Hydroxytamoxifen. § shBAG3 vs. shSCR. */§: $p < 0.05$, **/§§: $p < 0.01$, ***/§§§:

421 $p < 0.001$, ns: no significance, as indicated.

422

422



423

424 Figure S11 **Reduced A β deposition following TBI in TG mice through autophagy.** A ROI of CC, EC,

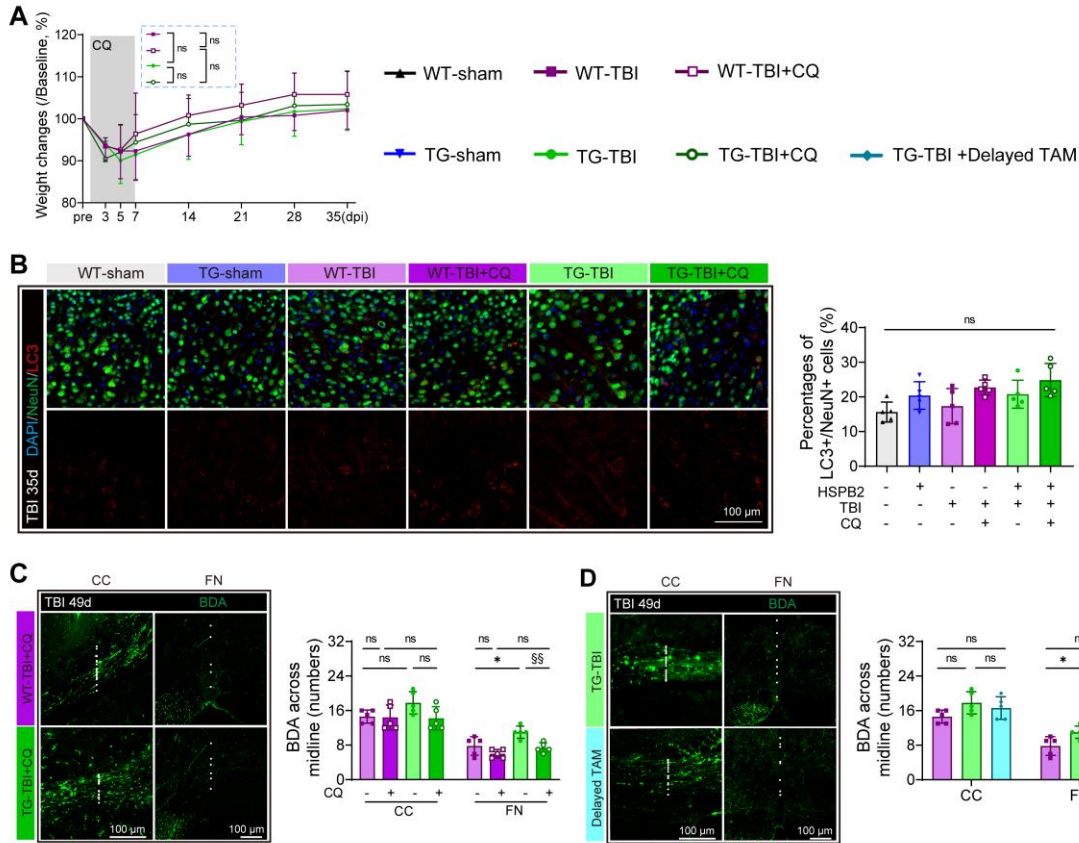
425 CTX, STR, and HIP; **B** Illustration of A β aggregation in cortex, corpus callosum, external capsule, striatum

426 and hippocampus with or without CQ at 3 days post-injury, dotted boxes indicate ROI, boxes indicate

427 enlarged area, blue: DAPI, green: NeuN, red: A β ; **C** Quantitative analysis of A β aggregation, n=4-5, analyzed

428 using one-way ANOVA and post hoc Bonferroni test. ns: no significance.

429



430

431 Figure S12 HSPB2's pro-recovery effects were reversed by acute-stage CQ administration or delayed
 432 induction. **A** Quantitative analysis of weight change from 3 to 35 days post-injury with CQ, n=15, 10, 17,
 433 10, respectively, analyzed using two-way ANOVA and post hoc Bonferroni test; **B** Illustration and
 434 quantitative analysis of LC3 levels in neurons in CTX after 35 days following TBI, blue: DAPI, green: NeuN,
 435 red: LC3, scale bar =100 μ m, n=5, analyzed using one-way ANOVA and post hoc Bonferroni test;**C&D**
 436 Illustration and quantification of BDA fiber crossing midline in CC and FN at 49 days post-injury with CQ
 437 (c) or delayed TAM (d), scale bar = 100 μ m, n=5, analyzed using one-way ANOVA and post hoc Bonferroni
 438 test. * indicates TG vs. WT, § indicates CQ vs. without CQ or delayed vs. normal TAM. *: $p < 0.05$, ns: no
 439 significance, as indicated.

440 **Supplemental Tables**

441 **Table S1 Correlation matrix of DTI and behaviors**

442 Please see a file for the other supporting materials: Table.S1.xlsx

443

444 **Table S2 Docking prediction of β APP, HSPB2 and BAG3**

Protein A	Protein B	interface area, Å ²	Δ iG, kcal/mol	Δ iG P-value
APP	HSPB2	2596.6	-32.4	0.345
BAG3	HSPB2	2113.4	-18.0	0.550

445 Protein structures were obtained from AlphaFold, HSPB2: AF-Q16082-F1, APP: AF-P05067-F1, BAG3: AF-

446 O95817-F1; docking was predicted by GRAMM-X, method: rigid docking; interactions were quantified by

447 PDBePISA

448

449

450 **Table S3 Correlation matrix of autophagy vesicles, foot-fault rates and β APP accumulation**

451 Please see a file for the other supporting materials: Table.S3.xlsx

452

453 **Table S4 Statistical analysis**

454 Please see a file for the other supporting materials: Table.S4.docx

455

456 **Supplemental Movies**

457 **Movie S1. HSPB2 increased the fiber tracts across the middle of CC at day 49.** The representative 3D
458 structures of the projection of the fiber tracts across the middle of CC of WT-TBI and TG-TBI mice at 49
459 days post injury, using the software DSI-studio.

460 Please see a file for the other supporting materials: Movie. S1.mp4

461 **Movie S2 Calcium fiber photometry recording.** The process of calcium fiber photometry recording when
462 stimulating each forepaw and their calcium responses.

463 Please see a file for the other supporting materials: Movie. S2.mp4

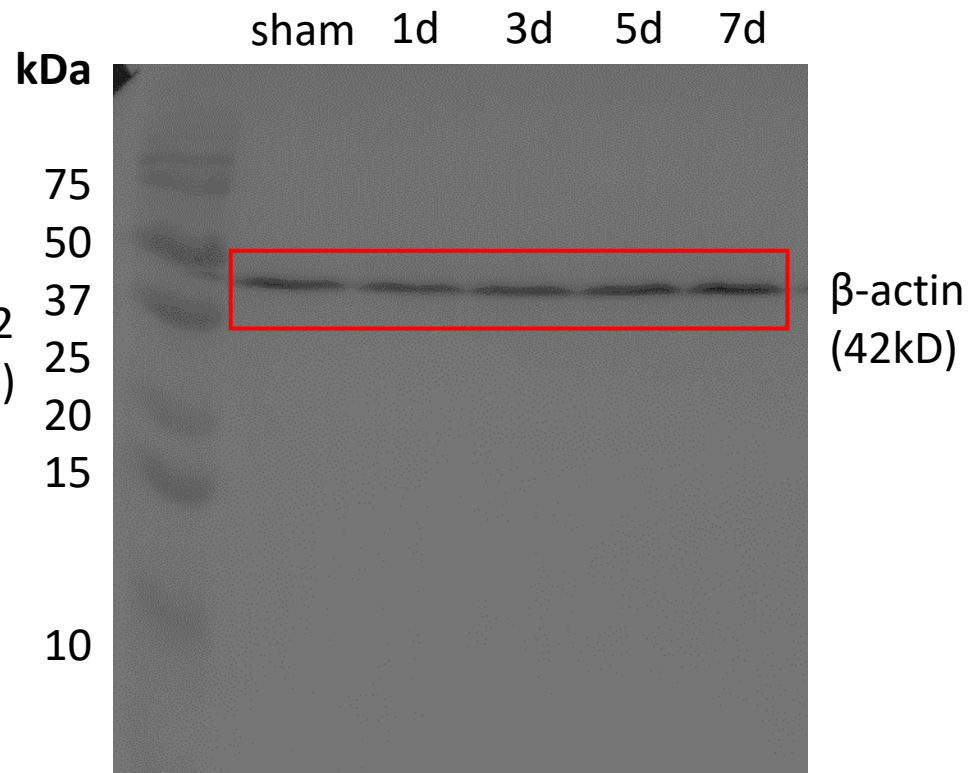
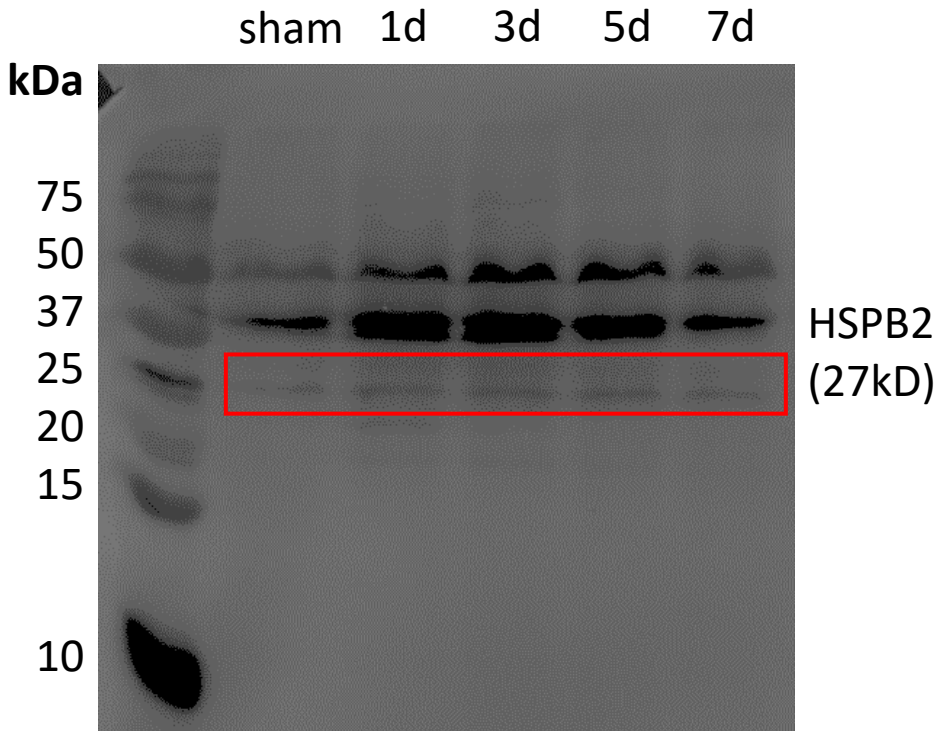
464

466 **Supplemental References**

- 467 1. G. Wang *et al.*, Scriptaid, a novel histone deacetylase inhibitor, protects against traumatic brain
468 injury via modulation of PTEN and AKT pathway : scriptaid protects against TBI via AKT.
469 *Neurotherapeutics* **10**, 124-142 (2013).
- 470 2. Y. Zhao *et al.*, Microglia-specific deletion of histone deacetylase 3 promotes inflammation
471 resolution, white matter integrity, and functional recovery in a mouse model of traumatic brain injury.
472 *J Neuroinflammation* **19**, 201 (2022).
- 473 3. A. M. A. Anthony Jalin, R. Jin, M. Wang, G. Li, EPPS treatment attenuates traumatic brain injury
474 in mice by reducing A² burden and ameliorating neuronal autophagic flux. *Experimental neurology*
475 **314**, 20-33 (2019).
- 476 4. P. M. Washington *et al.*, The effect of injury severity on behavior: a phenotypic study of cognitive
477 and emotional deficits after mild, moderate, and severe controlled cortical impact injury in mice. *J*
478 *Neurotrauma* **29**, 2283-2296 (2012).
- 479 5. P. Wei *et al.*, Cordycepin confers long-term neuroprotection via inhibiting neutrophil infiltration and
480 neuroinflammation after traumatic brain injury. *J Neuroinflammation* **18**, 137 (2021).
- 481 6. X. Liu *et al.*, Interleukin-4 Is Essential for Microglia/Macrophage M2 Polarization and Long-Term
482 Recovery After Cerebral Ischemia. *Stroke* **47**, 498-504 (2016).
- 483 7. M.-Y. Xu, Y.-F. Wang, P.-J. Wei, Y.-Q. Gao, W.-T. Zhang, Hypoxic preconditioning improves long-
484 term functional outcomes after neonatal hypoxia-ischemic injury by restoring white matter integrity
485 and brain development. *Cns Neurosci Ther* **25**, 734-747 (2019).

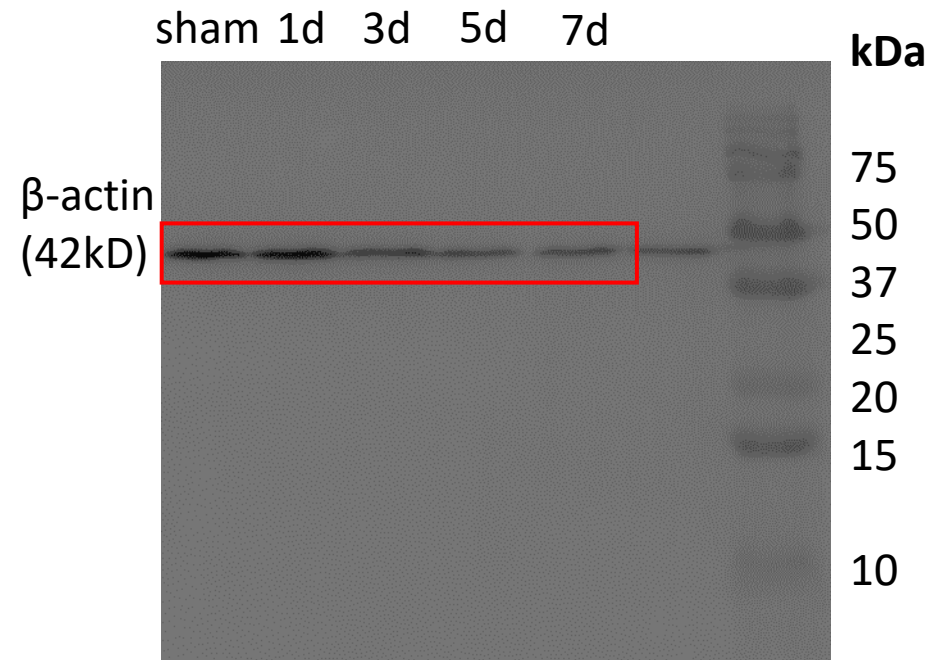
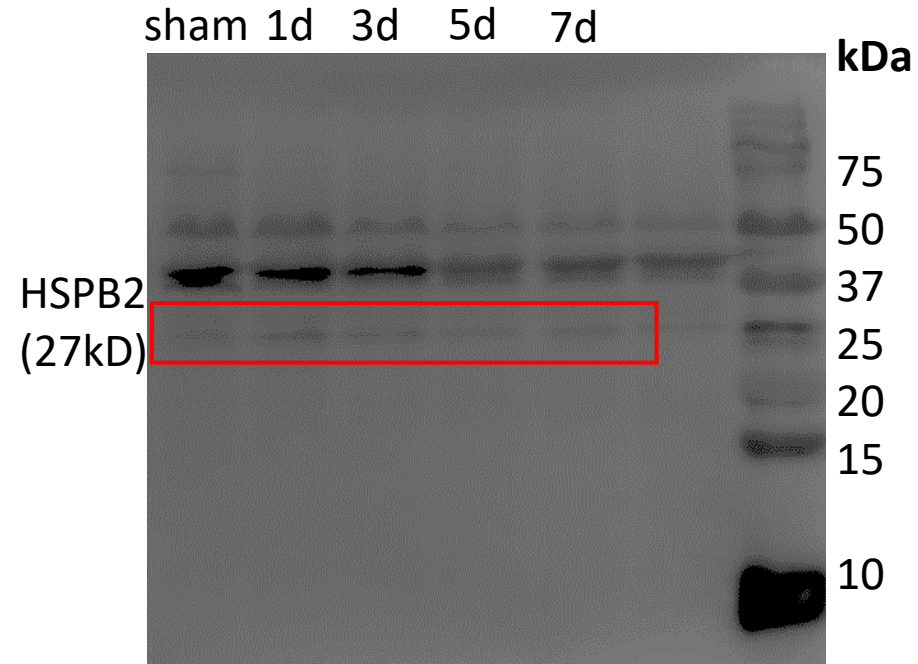
HSPB2 expression after TBI – CTX

Full unedited gel for **Figure.1B**



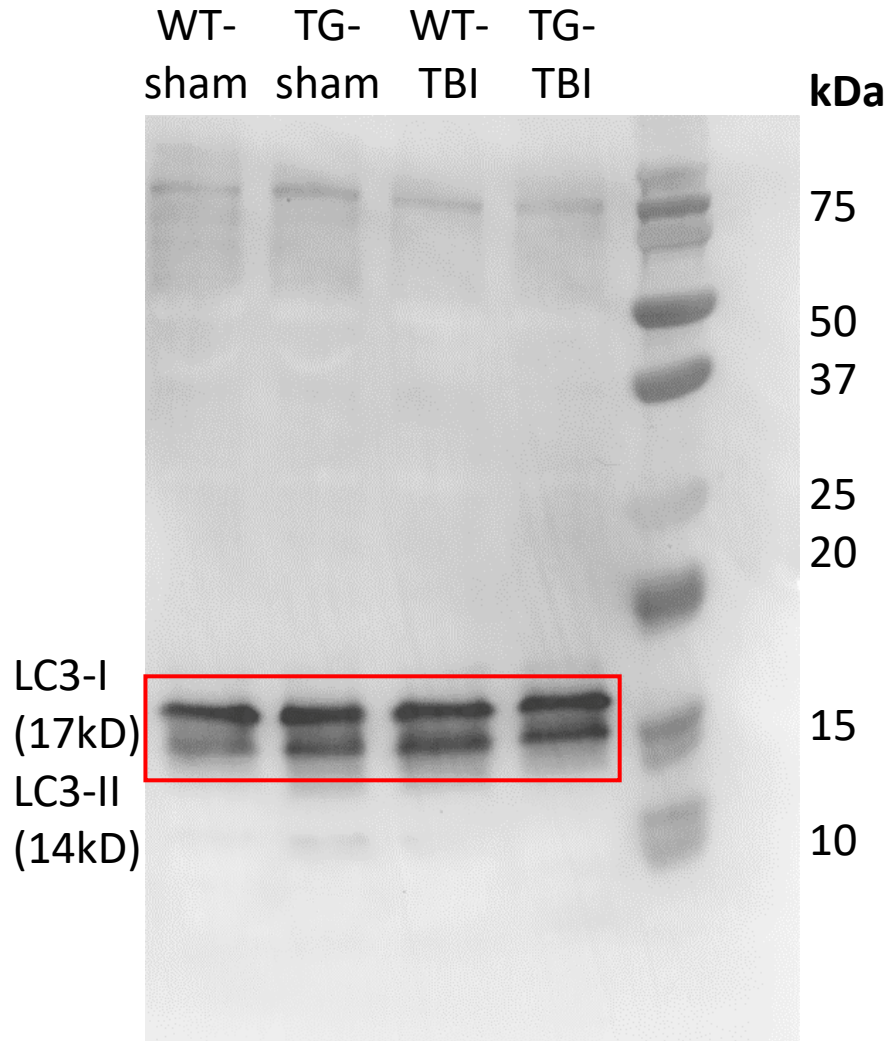
HSPB2 expression after TBI- HIP

Full unedited gel for **Figure.1B**



LC3 after TBI 3d

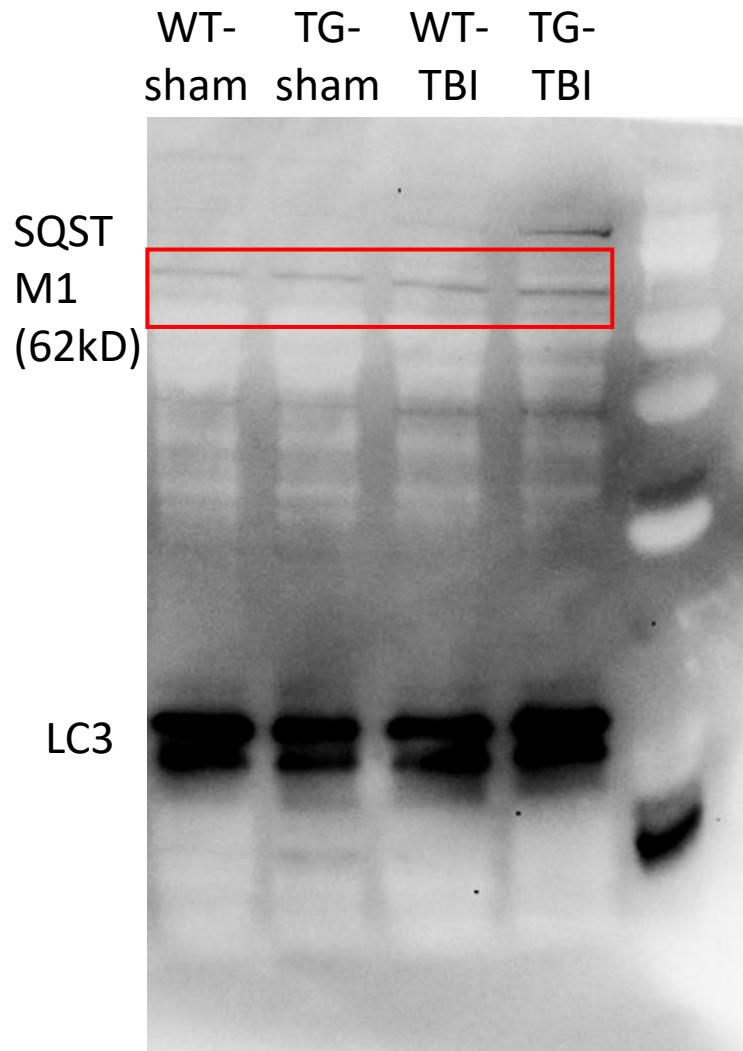
Full unedited gel for **Figure.7D**



On 15% SDS-PAGE

SQSTM1 after TBI 3d

Full unedited gel for Figure.7D



On 15% SDS-PAGE

kDa

75

50

37

25

20

15

10

WT- sham TG- sham WT- TBI TG- TBI

β -actin (42kD)

kDa

75

50

37

25

20

15

10

stripped after "LC3 after TBI"

SQSTM1 after TBI+CQ 3d

WT- WT- TG- TG-
TBI TBI+CQ TBI TBI+CQ

kDa

75

50

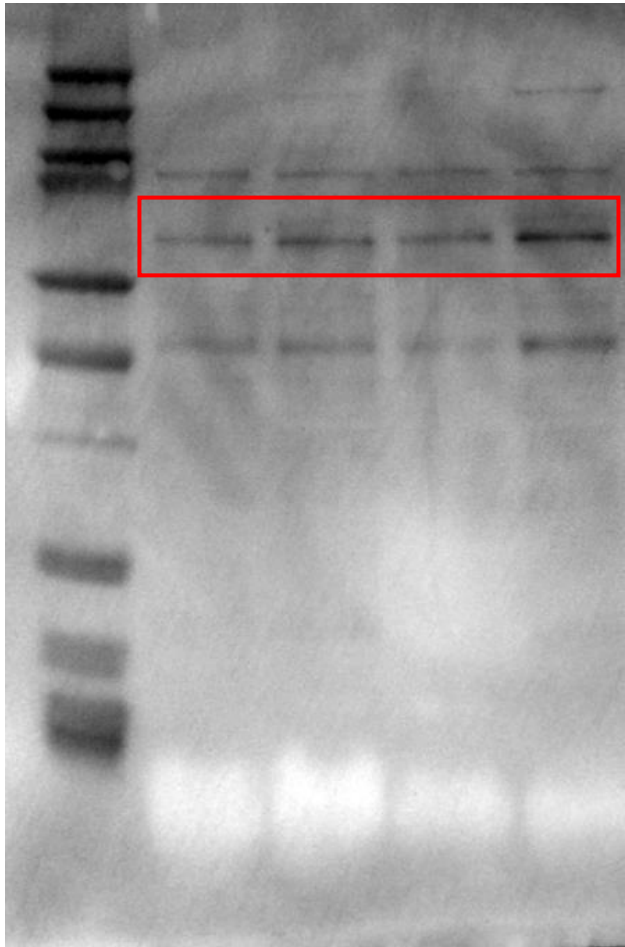
37

25

20

15

10



SQSTM
M1
(62kD)

On 15% SDS-PAGE

Full unedited gel for Figure. 7E

WT- WT- TG- TG-
TBI TBI+CQ TBI TBI+CQ

kDa

75

50

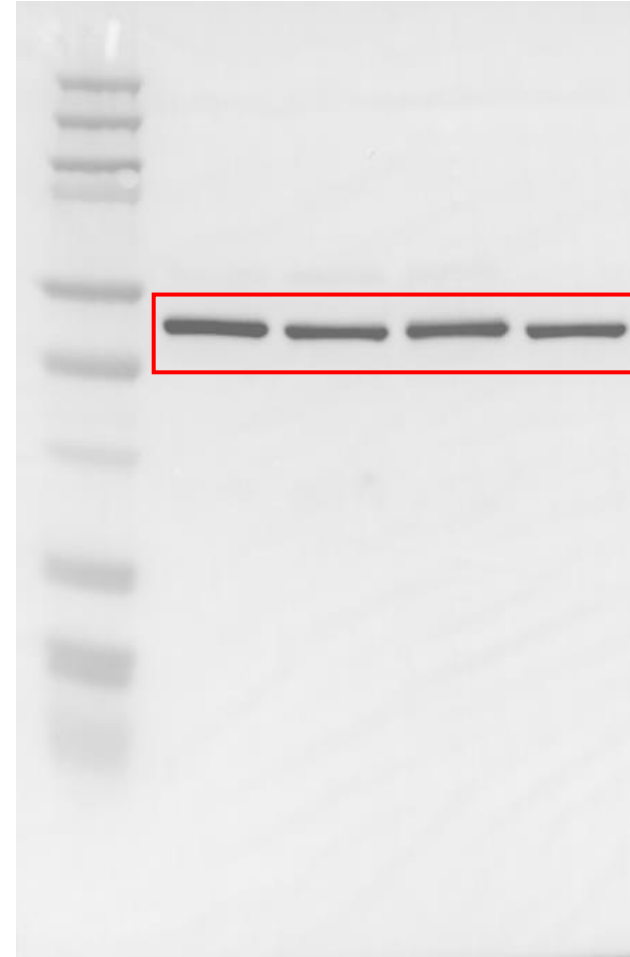
37

25

20

15

10



β -actin
(42kD)

LC3 after TBI+CQ 3d

Full unedited gel for **Figure.7E**

WT- WT- TG- TG-
TBI TBI+CQ TBI TBI+CQ

kDa

75

50

37

25

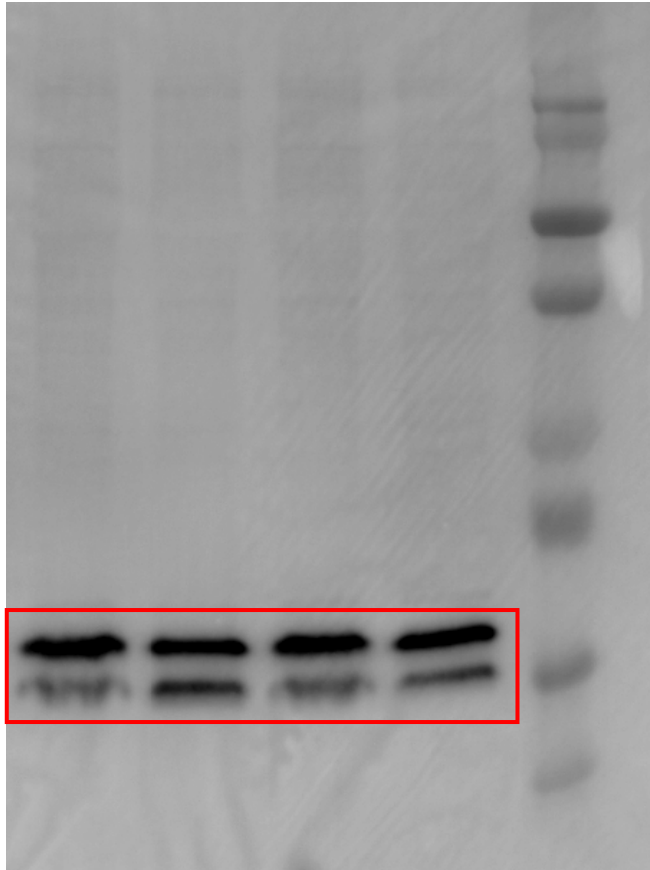
20

15

10

LC3-I
(17kD)

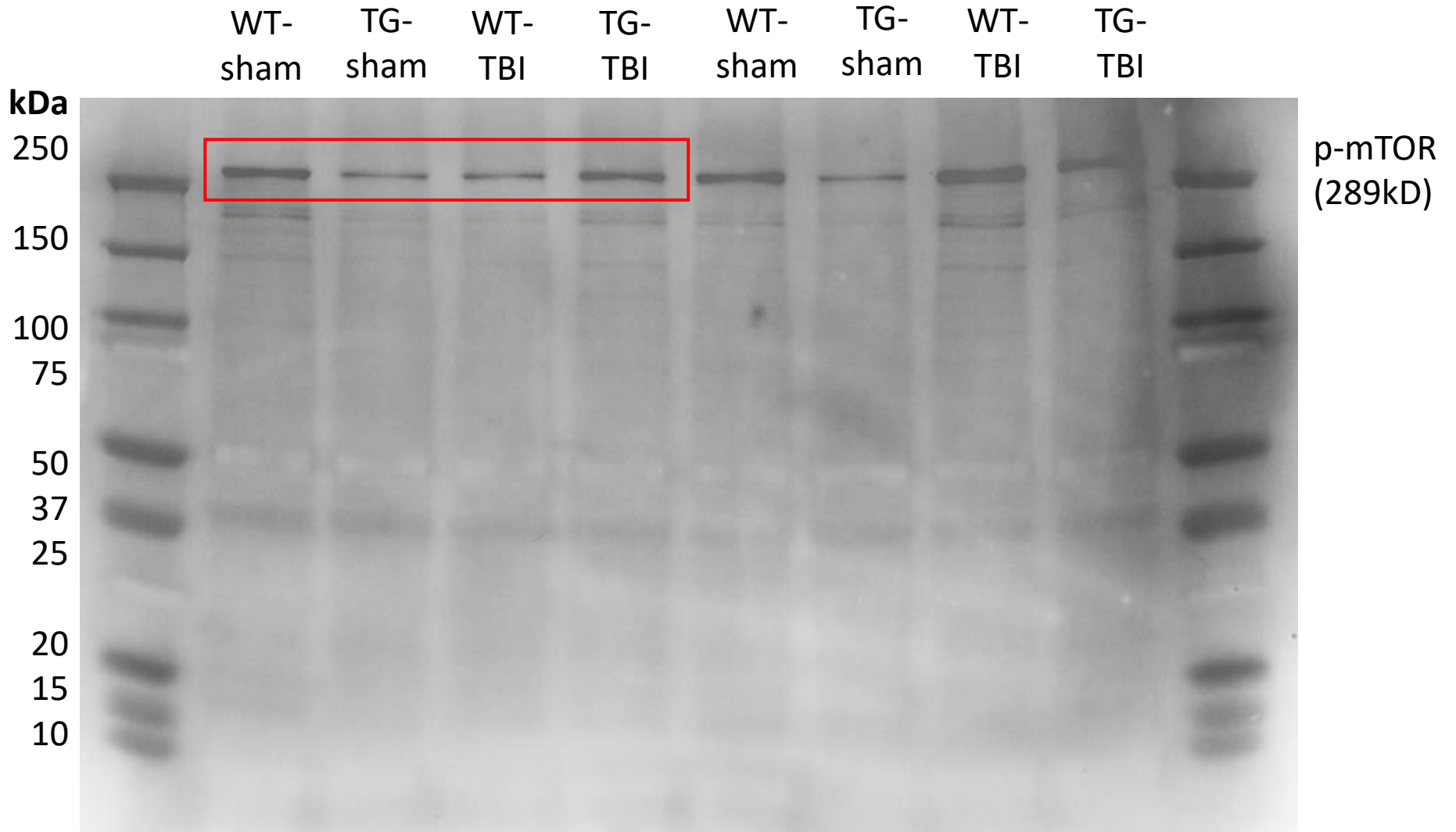
LC3-II
(14kD)



On 15% SDS-PAGE

p-mTOR/mTOR after TBI 3d

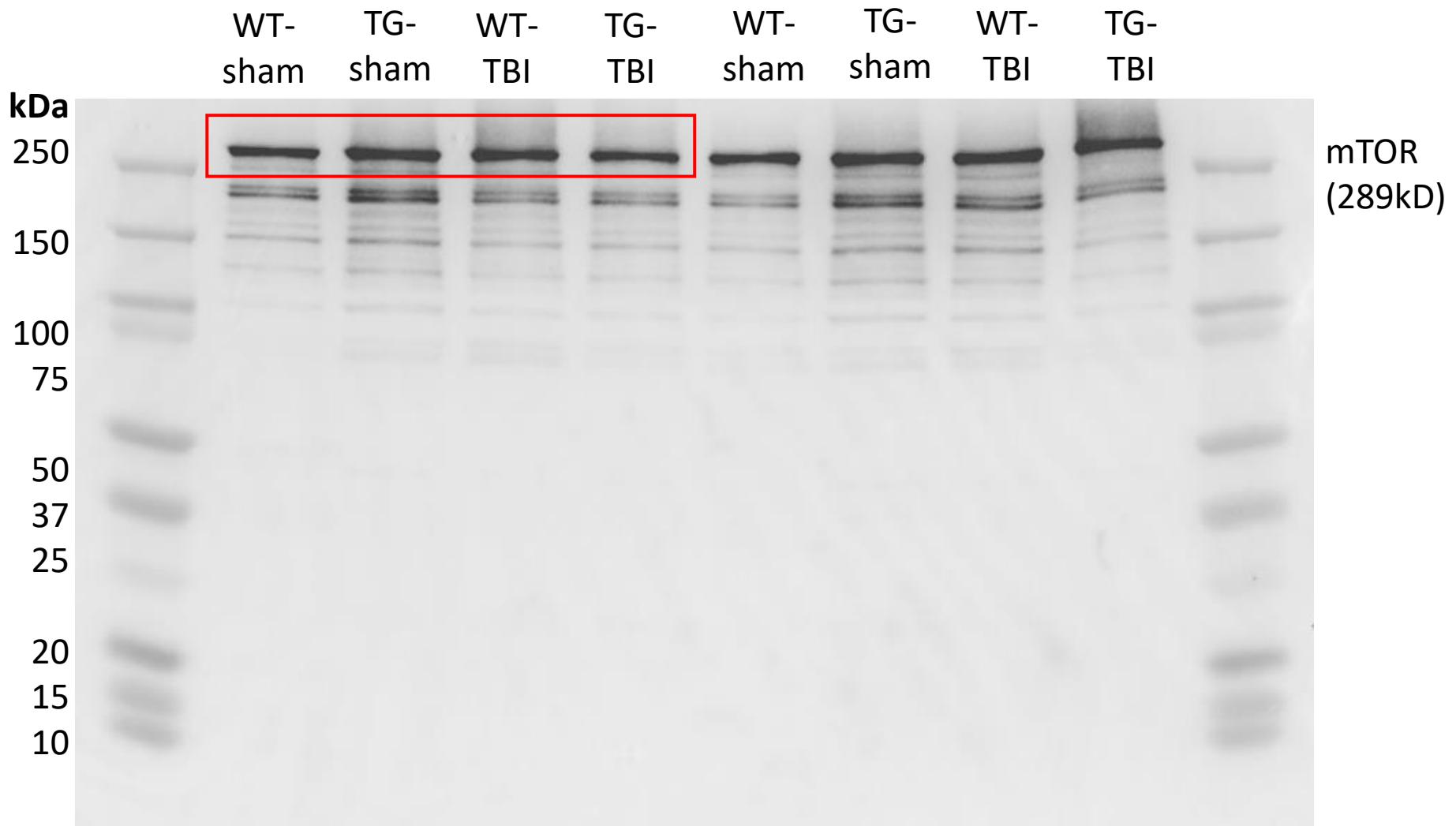
Full unedited gel for **Figure.9B**



On 4-20% SDS-PAGE

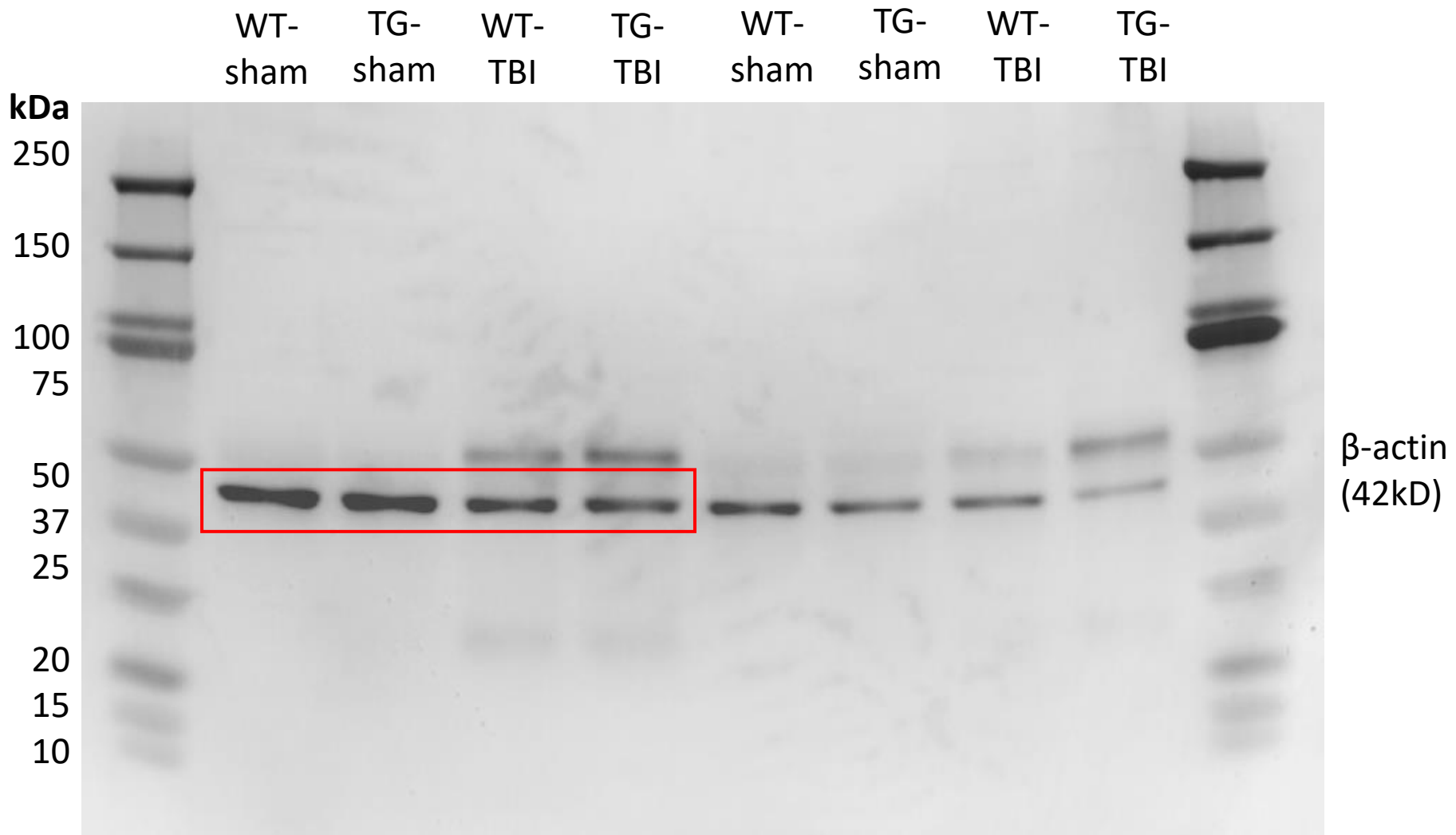
p-mTOR/mTOR after TBI 3d

Full unedited gel for **Figure.9B**



On 4-20% SDS-PAGE

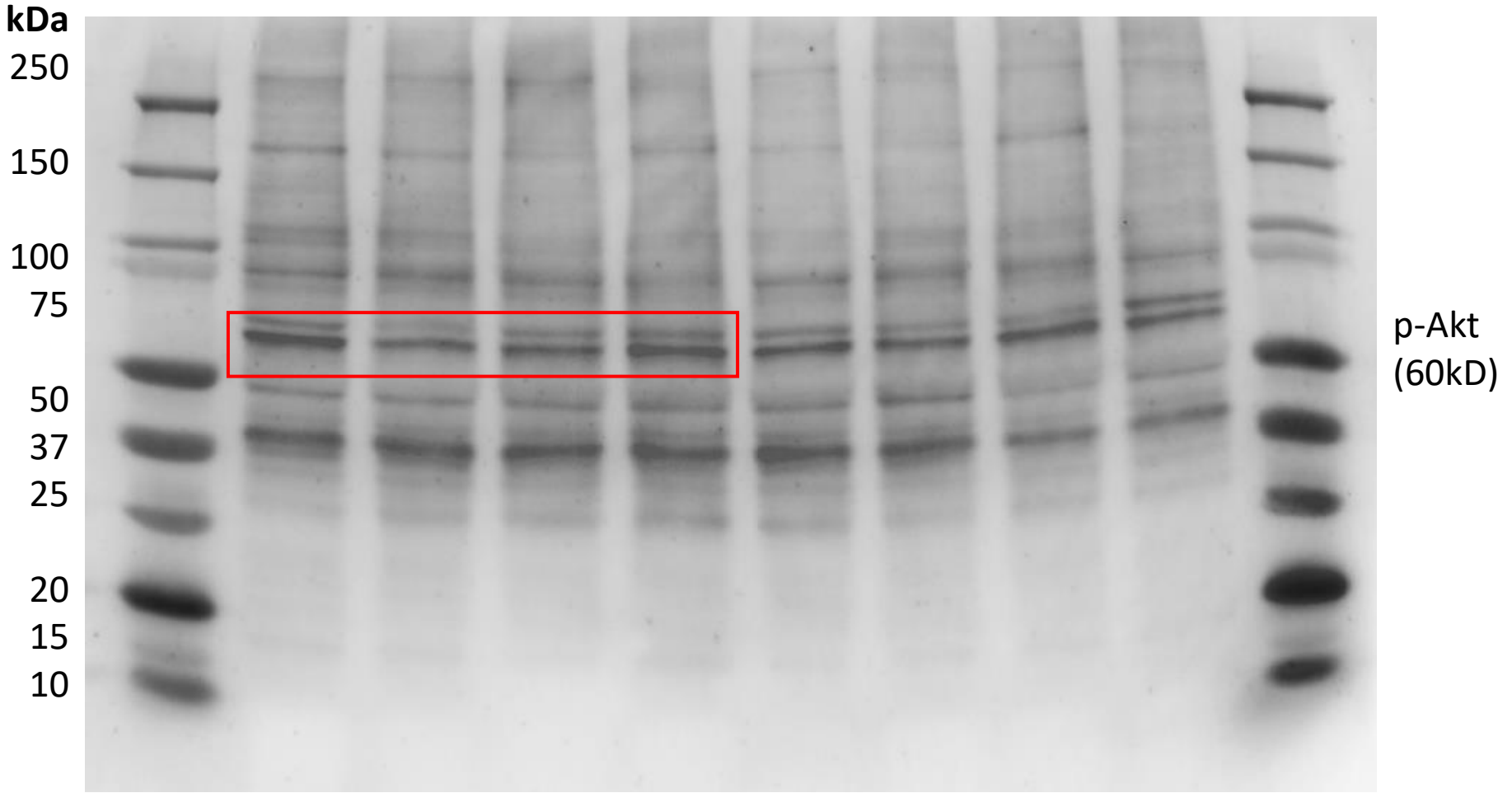
stripped after “**p-mTOR after TBI 3d**”



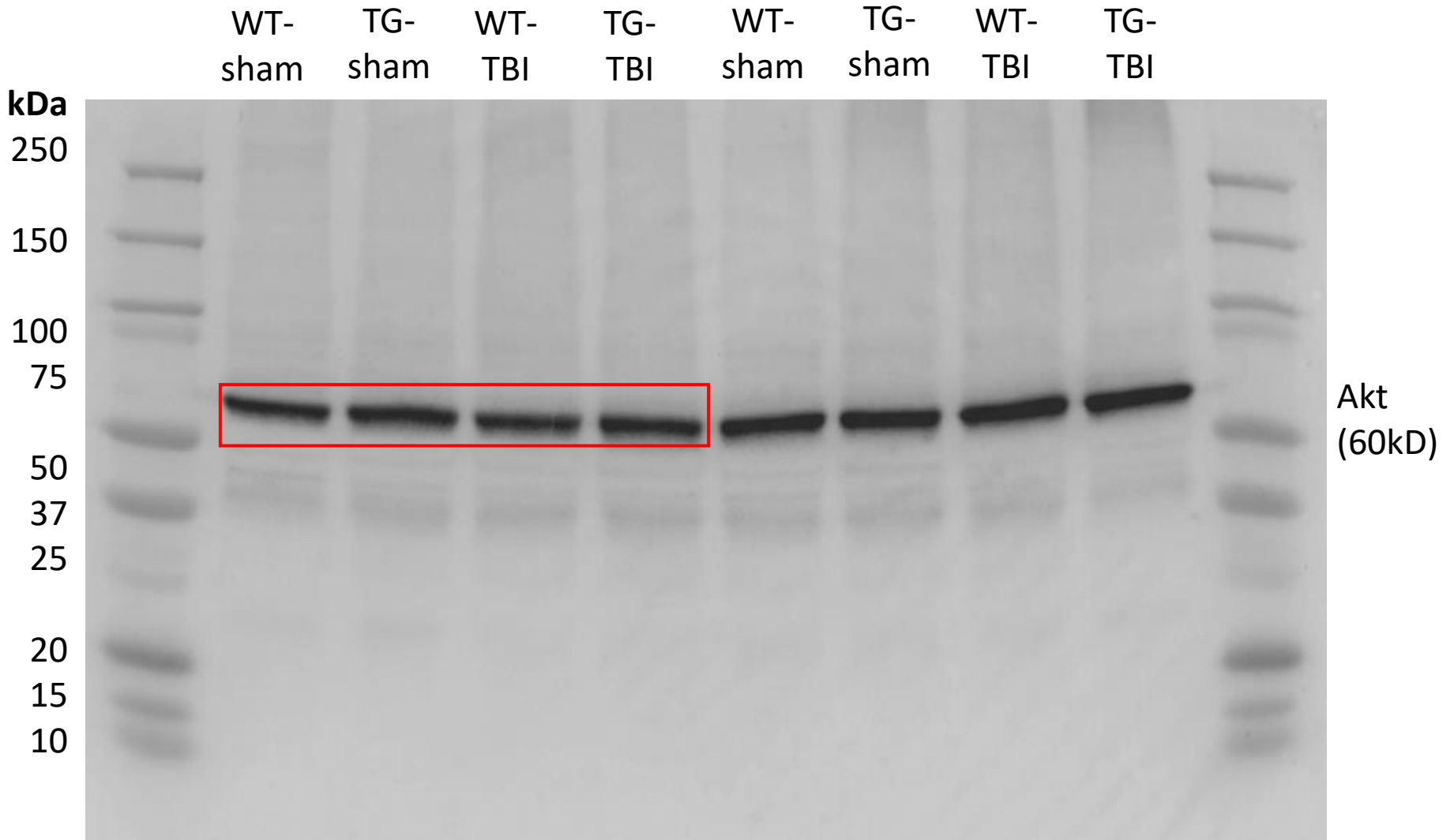
p-Akt/Akt after TBI 3d

Full unedited gel for **Figure.9B**

WT- sham TG- sham WT- TBI TG- TBI WT- sham TG- sham WT- TBI TG- TBI

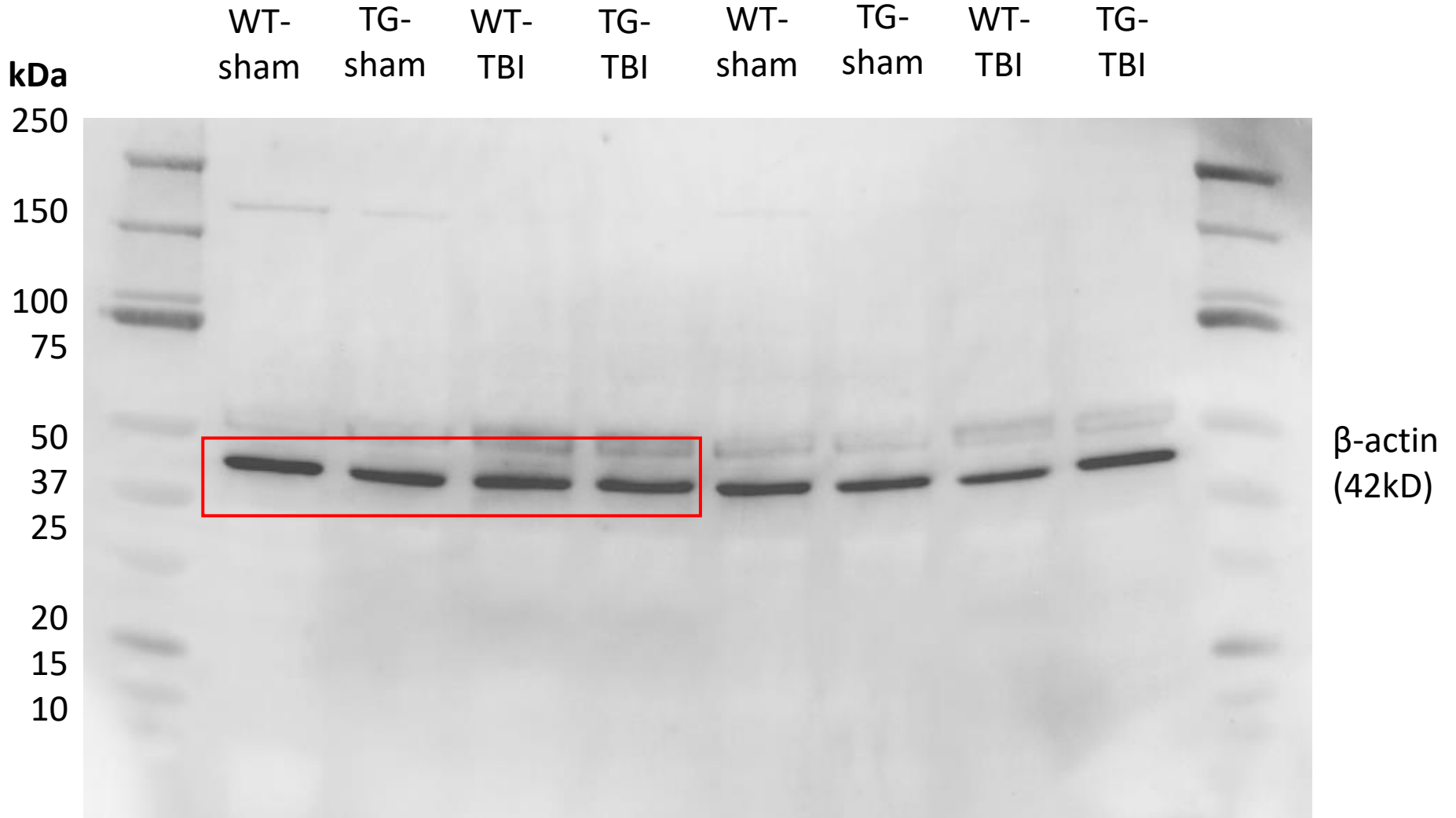


On 4-20% SDS-PAGE



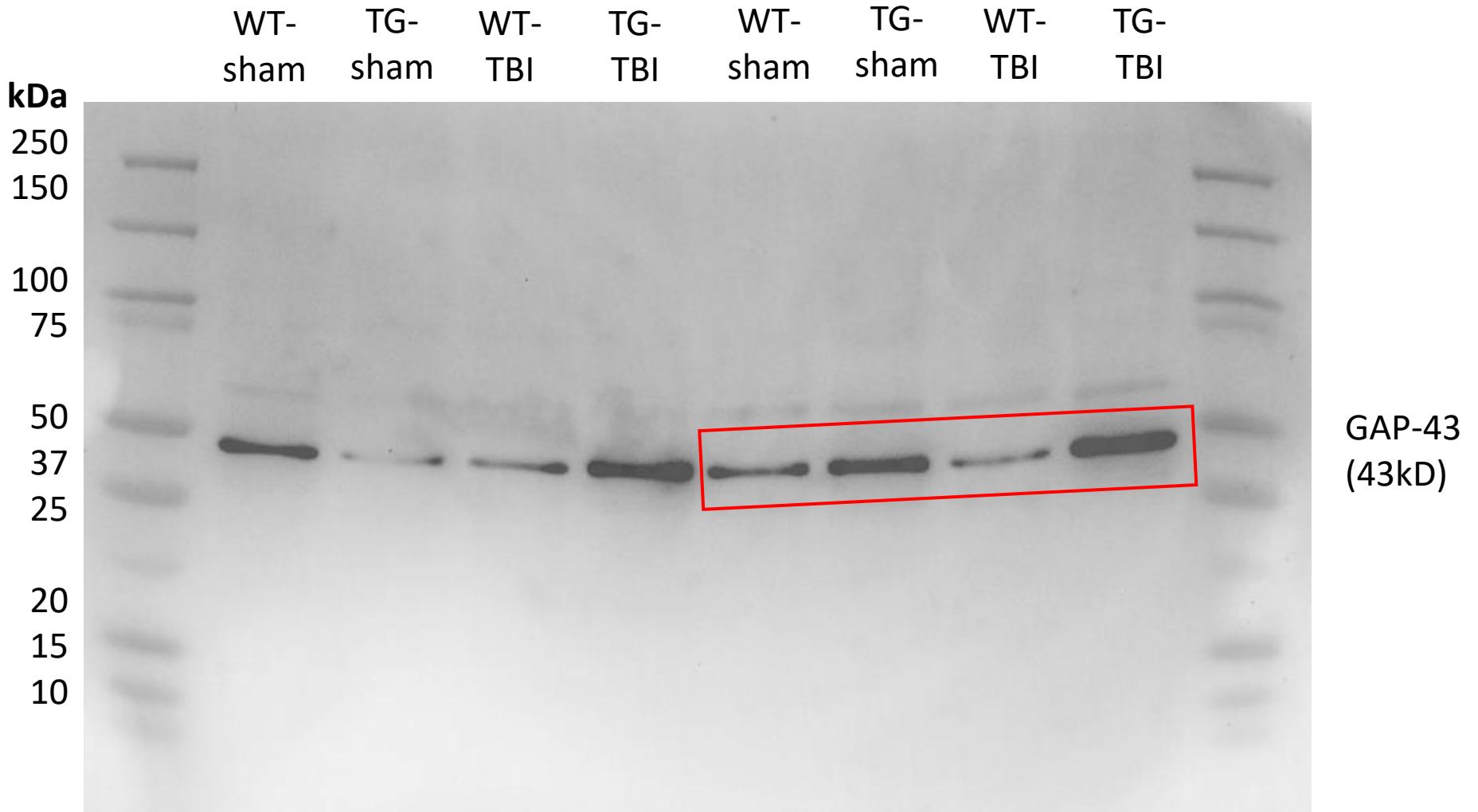
p-Akt/Akt after TBI 3d

Full unedited gel for **Figure.9B**



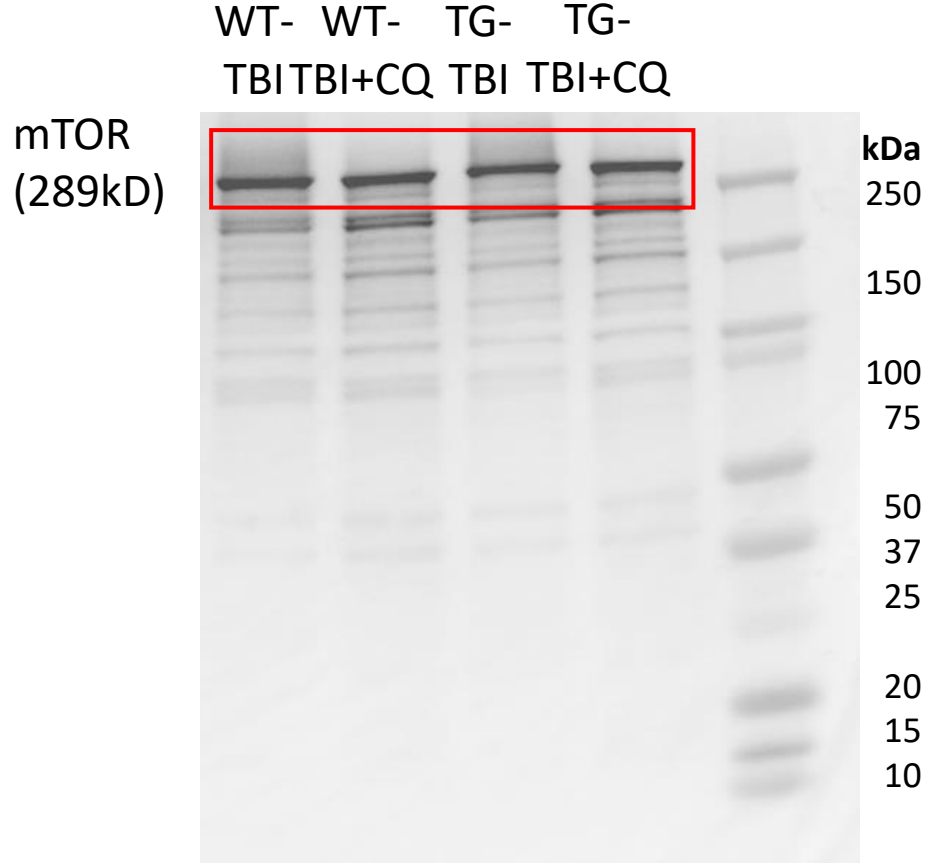
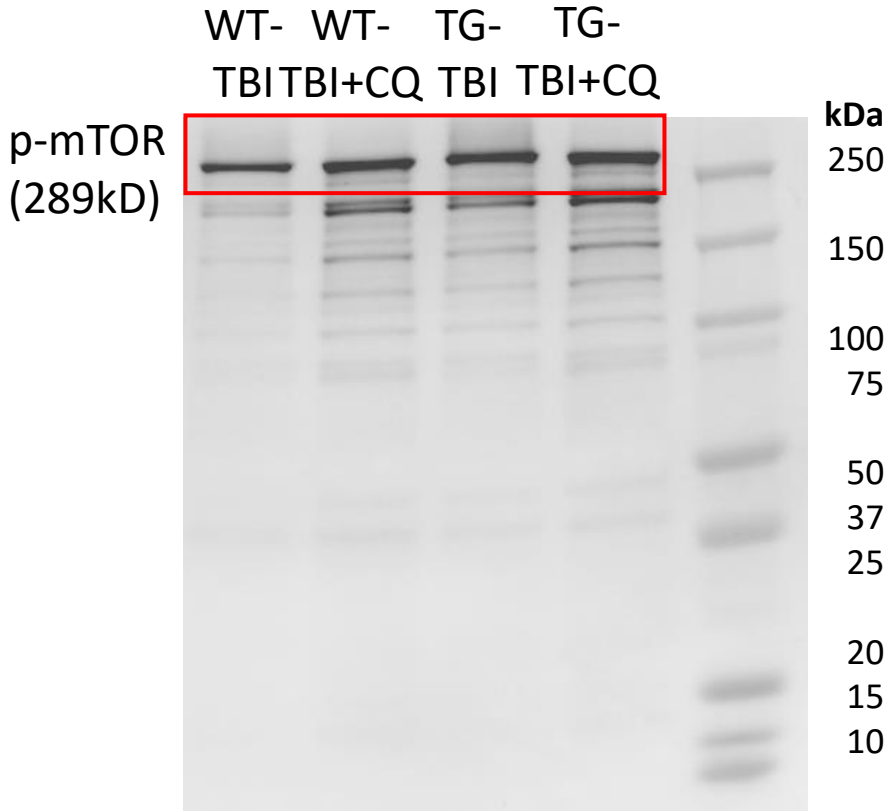
On 4-20% SDS-PAGE

stripped after "**p-Akt/Akt after TBI 3d**"



p-mTOR/mTOR after TBI +CQ 3d

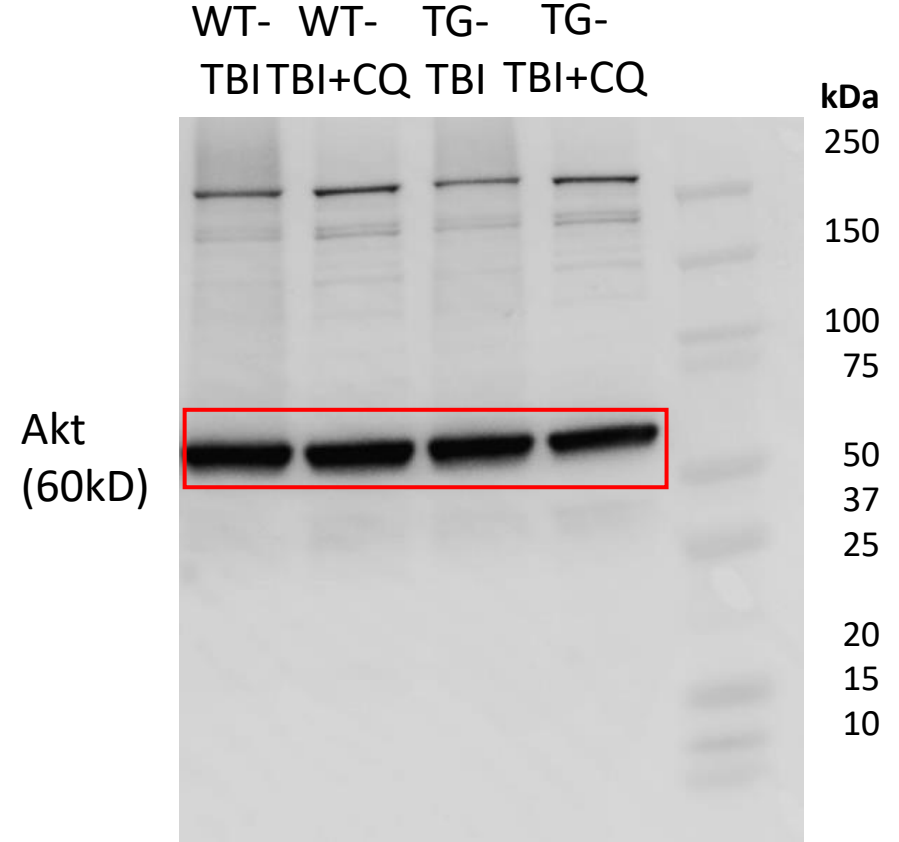
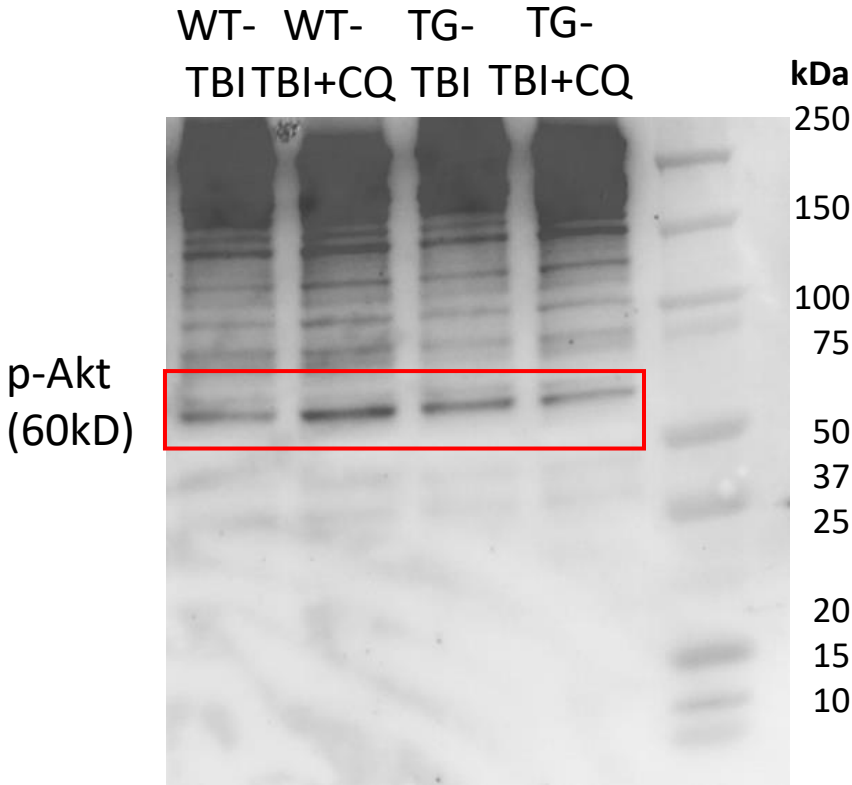
Full unedited gel for **Figure.9D**



On 4-20% SDS-PAGE stripped after “p-mTOR/mTOR after TBI +CQ 3d”

p-Akt/Akt after TBI +CQ 3d

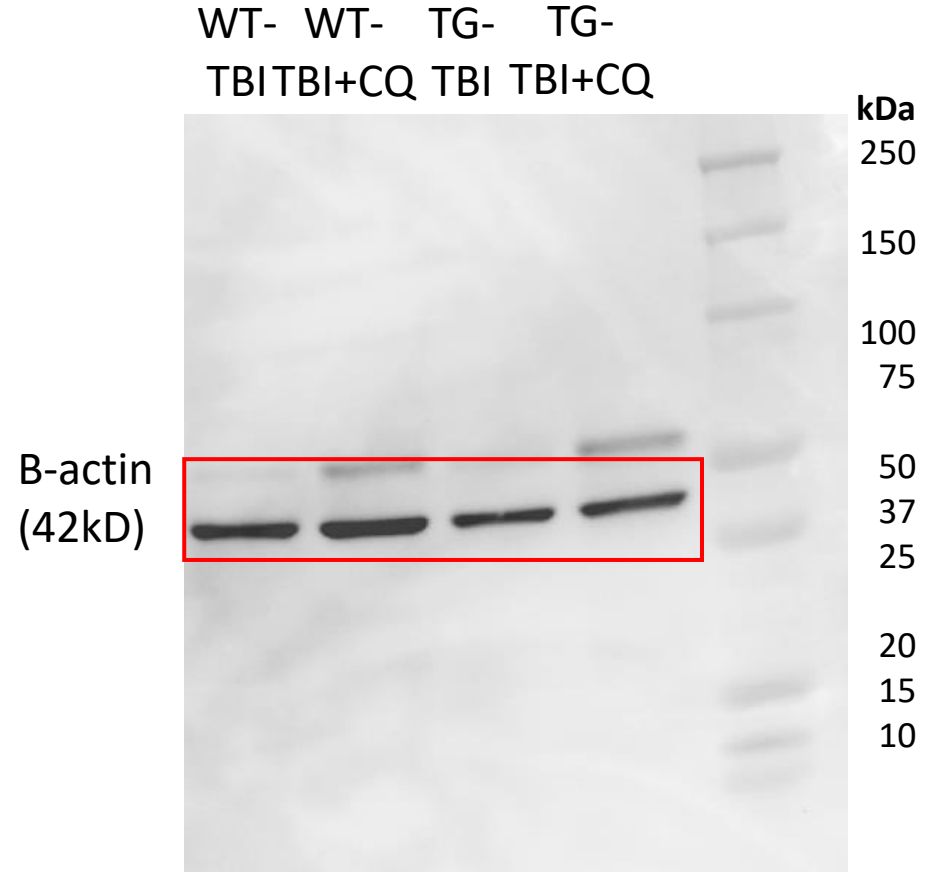
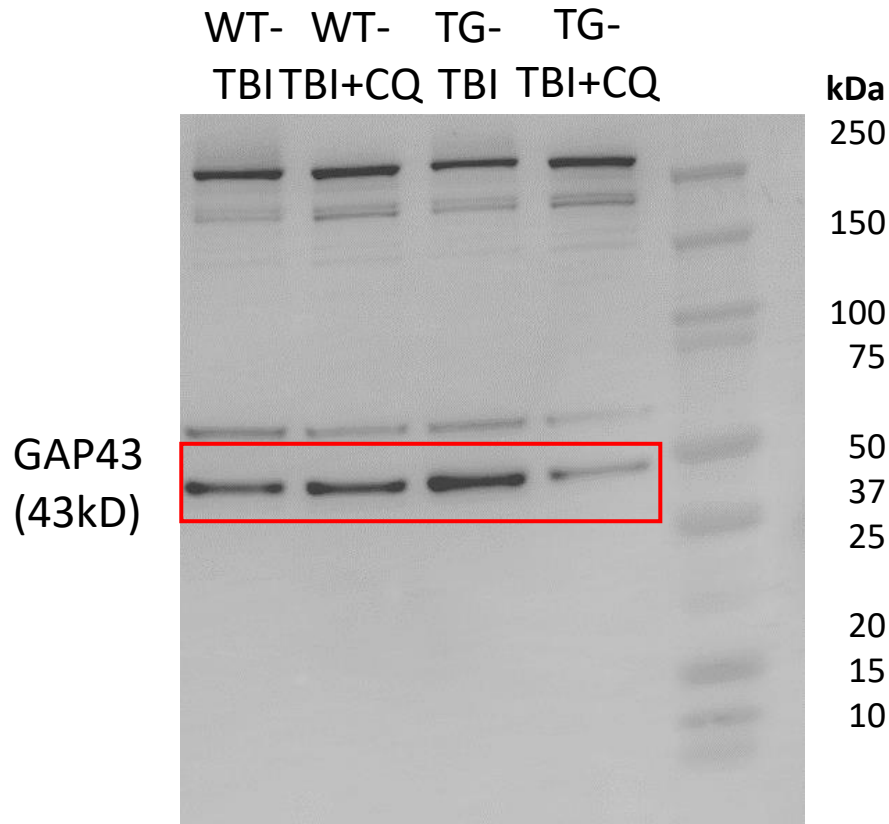
Full unedited gel for **Figure.9D**



On 4-20% SDS-PAGE stripped after “p-mTOR/mTOR after TBI +CQ 3d”

GAP43 after TBI +CQ 3d

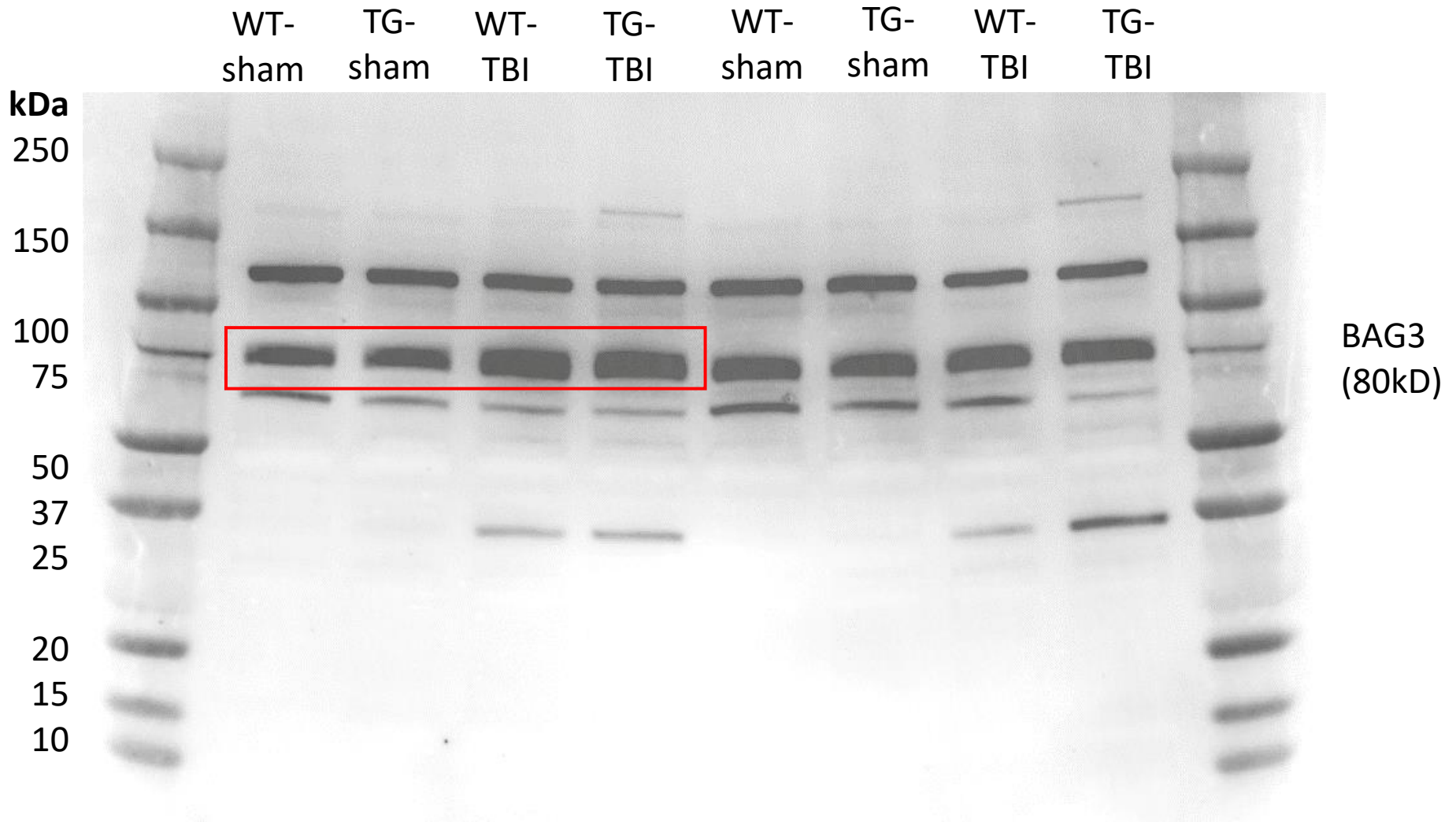
Full unedited gel for **Figure.9D**



On 4-20% SDS-PAGE stripped after "p-mTOR/mTOR after TBI +CQ 3d"

BAG3 after TBI +CQ 3d

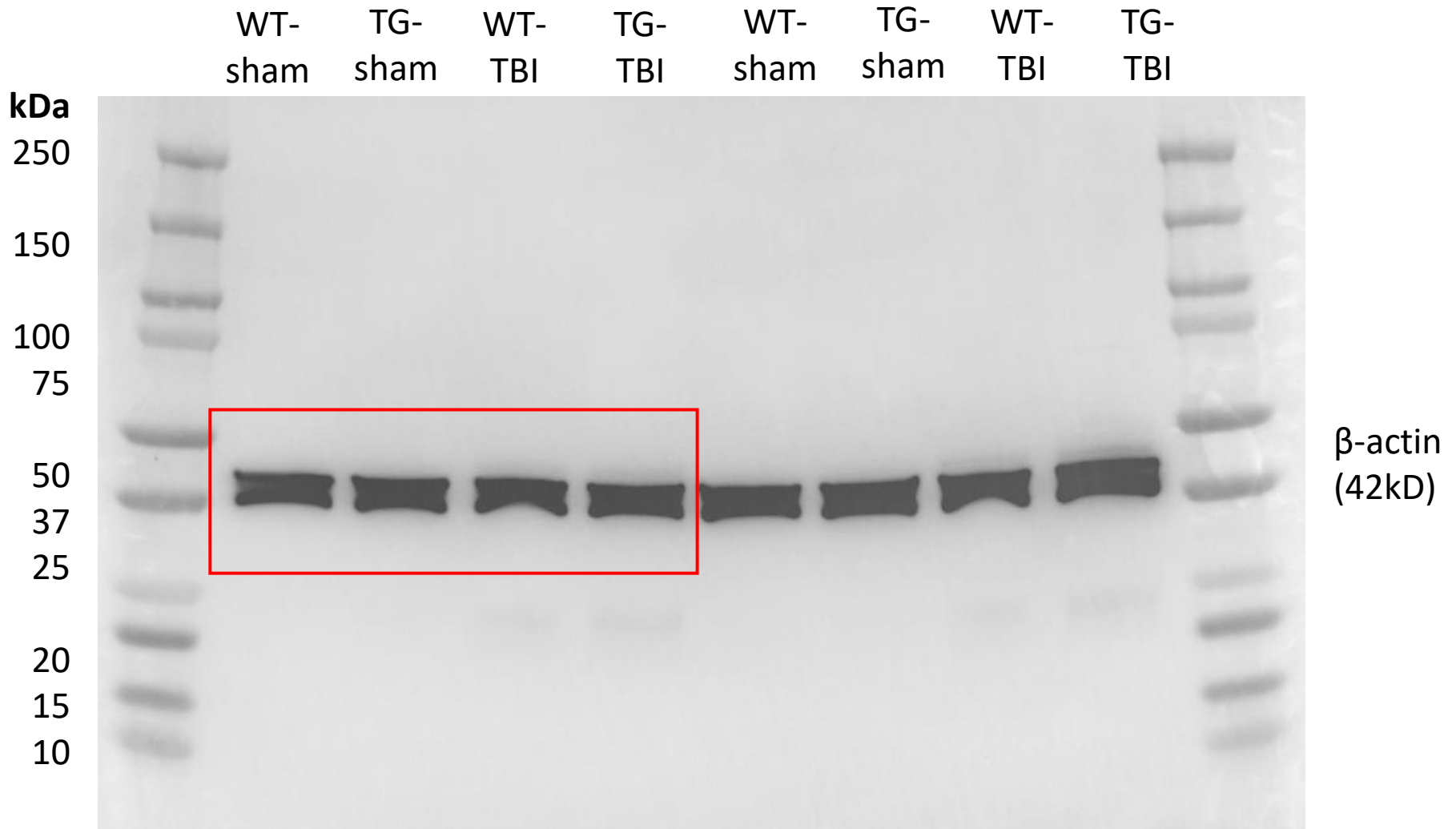
Full unedited gel for **Figure.10B**



On 4-20% SDS-PAGE

BAG3 after TBI +CQ 3d

Full unedited gel for **Figure.10B**



On 4-20% SDS-PAGE

stripped after "BAG3 after TBI +CQ 3d"

CoIP— β APP

IP: HA-Tag

Full unedited gel for **Figure.10D**
Input

IgG

CL

IL

IgG

CL

IL

kDa

250

150

100

75

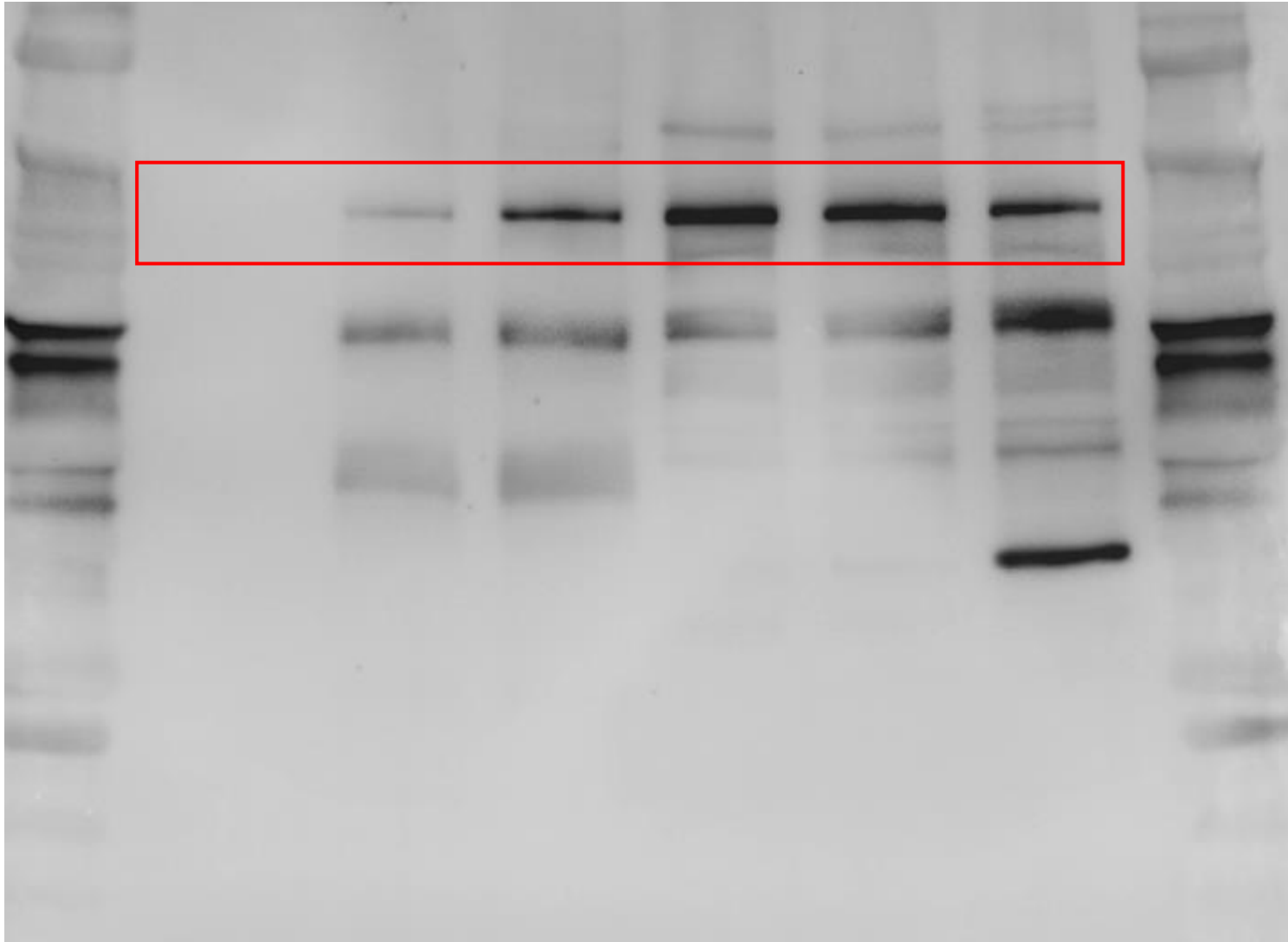
50

37

25

20

15



IB:
 β APP
(100kD)

CoIP—BAG3

IP: HA-Tag

Full unedited gel for Figure.10D
Input

kDa

IgG

CL

IL

IgG

CL

IL

250

150

100

75

50

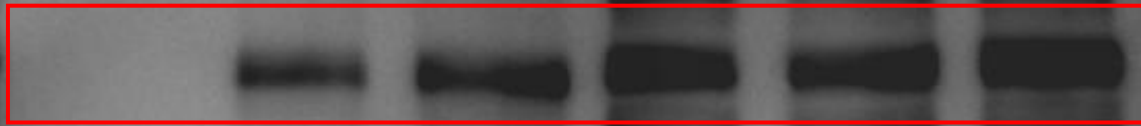
37

25

20

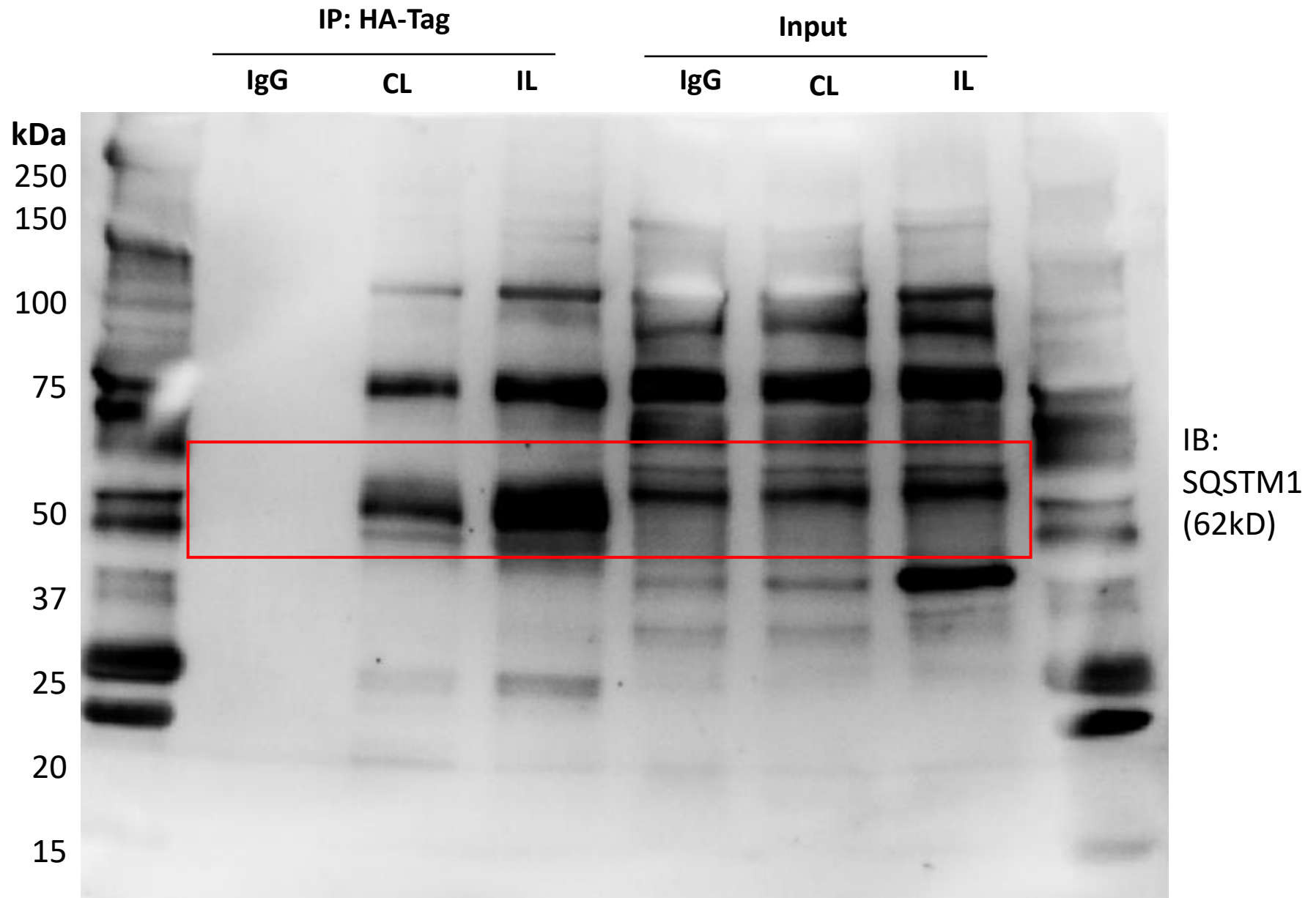
15

IB:
BAG3
(80kD)



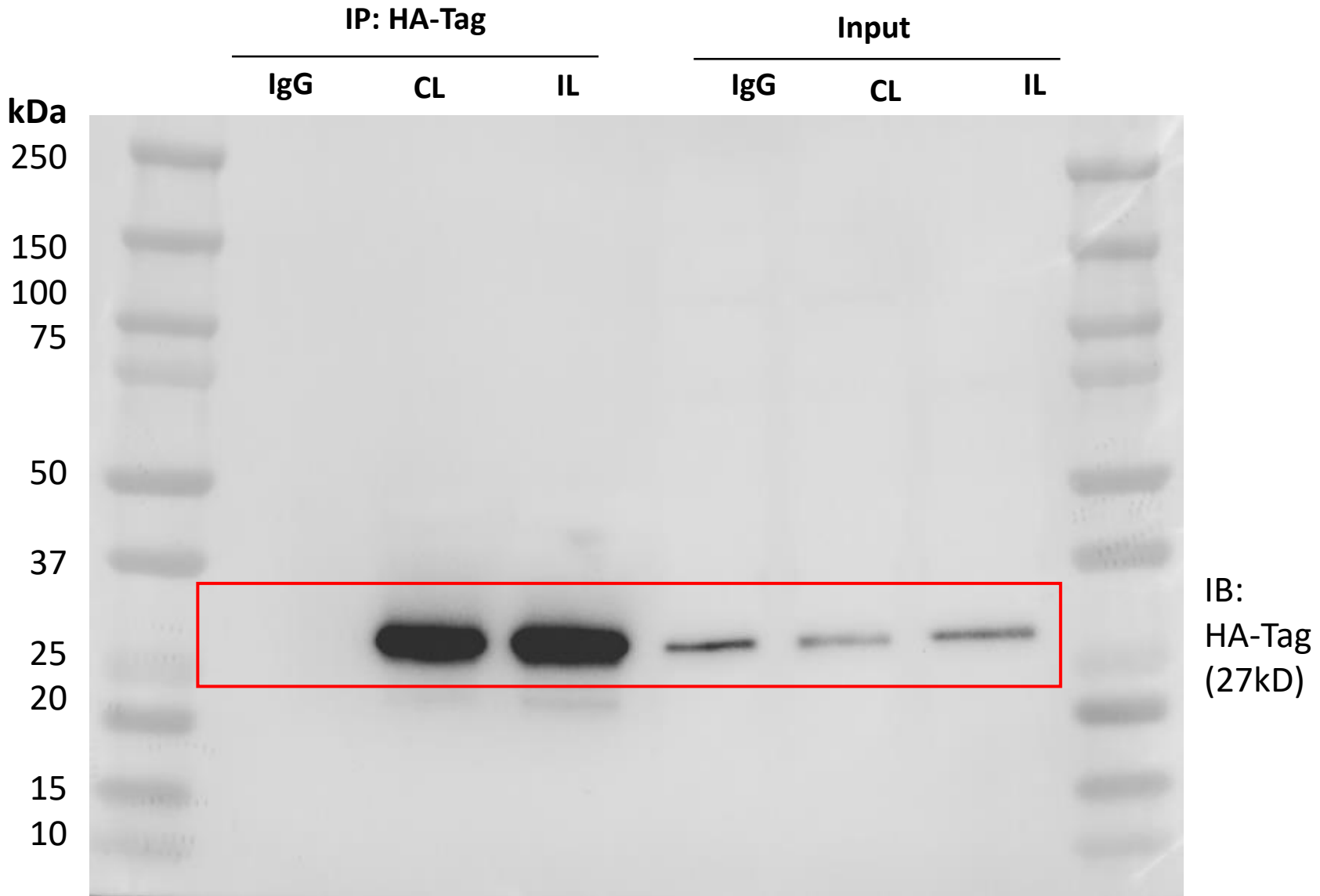
CoIP—SQSTM1

Full unedited gel for **Figure.10D**



On 10% SDS-PAGE

stripped after "CoIP—BAG3"



IB:
HA-Tag
(27kD)

CoIP—Akt

Full unedited gel for **Figure.10D**

IP: HA-Tag

Input

IgG

CL

IL

IgG

CL

IL

kDa

250

150

100

75

50

37

25

20

15

10

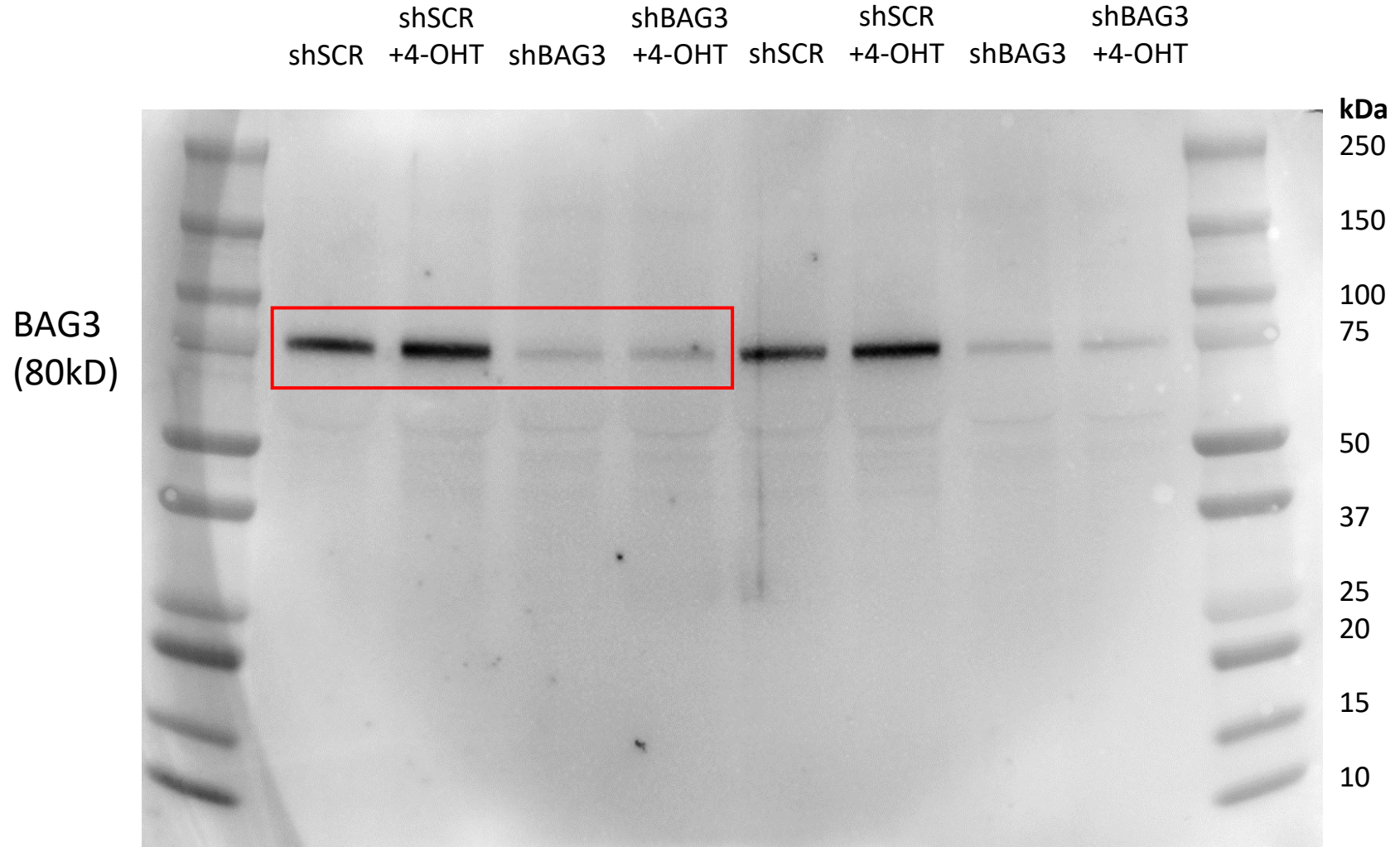
IB:
Akt
(60kD)

On 10% SDS-PAGE

stripped after "CoIP—HA-Tag"

BAG3 after OGD+shBAG3+4-OHT

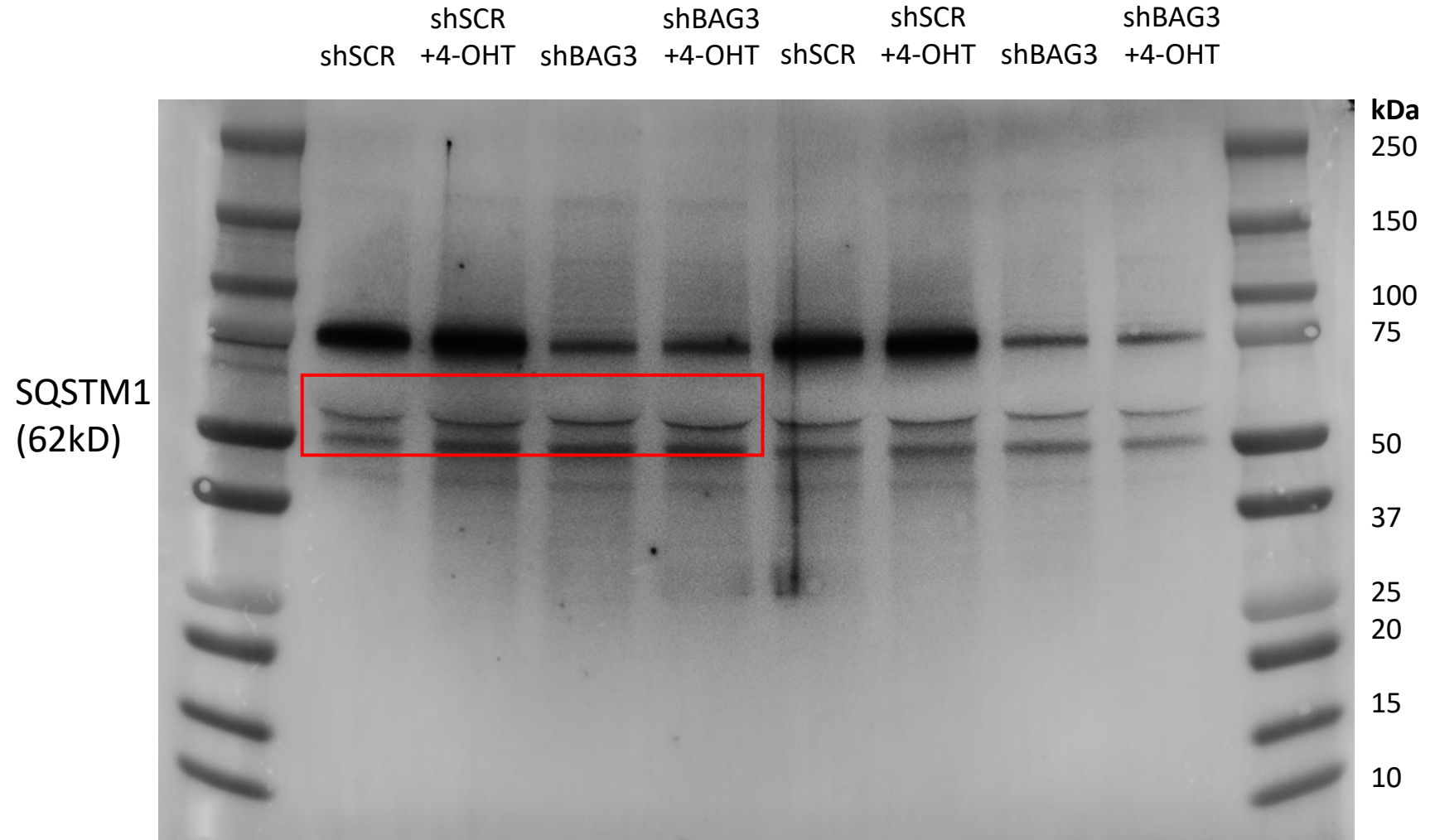
Full unedited gel for **Figure.11F**



On 4-20% SDS-PAGE

SQSTM1 after OGD+shBAG3+4-OHT

Full unedited gel for **Figure.11F**

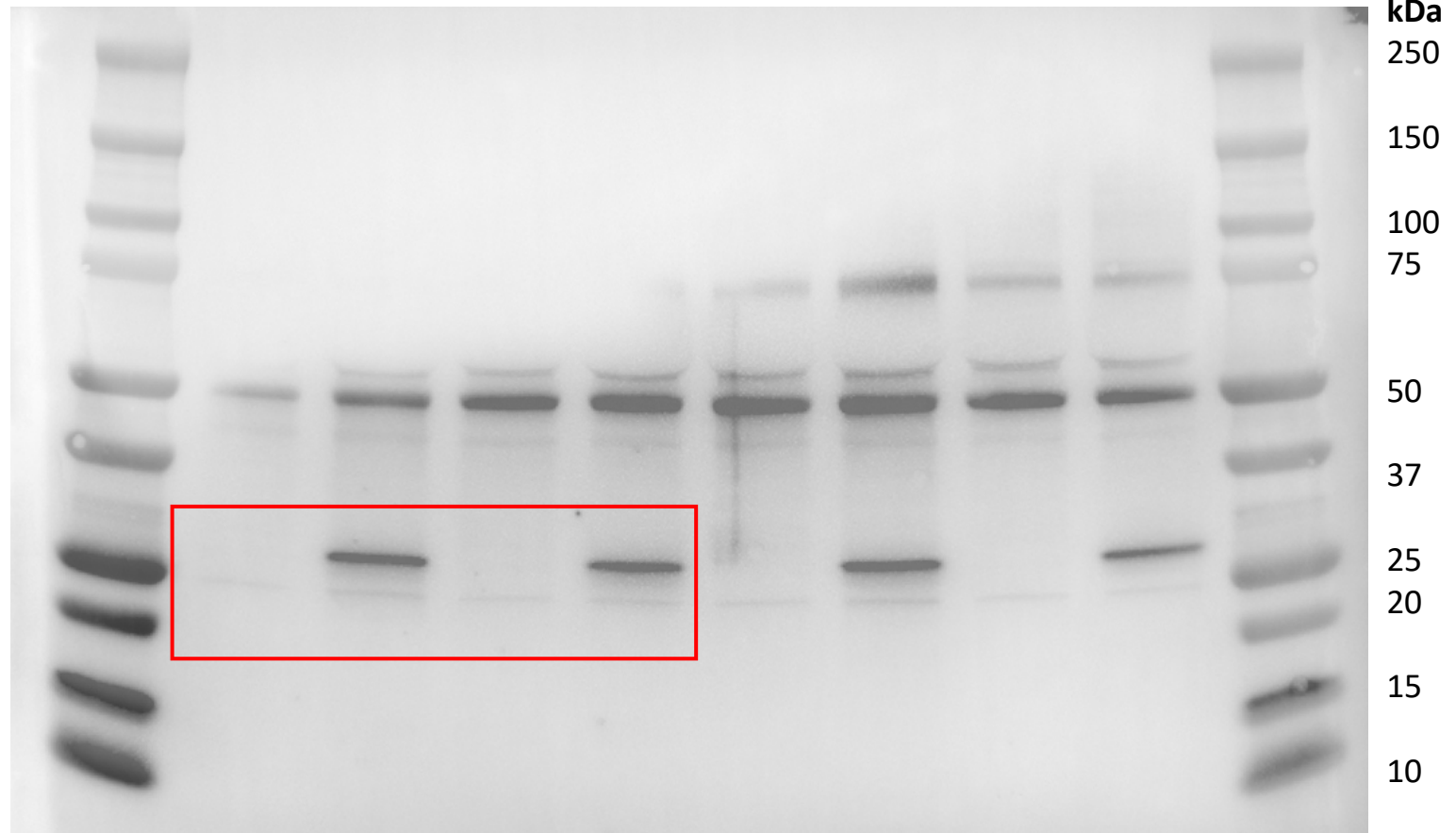


On 4-20% SDS-PAGE stripped after “**BAG3 after OGD+shBAG3+4-OHT**”

HSPB2 after OGD+shBAG3+4-OHT

Full unedited gel for **Figure.11F**

shSCR shBAG3 shSCR shBAG3
shSCR +4-OHT shBAG3 +4-OHT shSCR +4-OHT shBAG3 +4-OHT

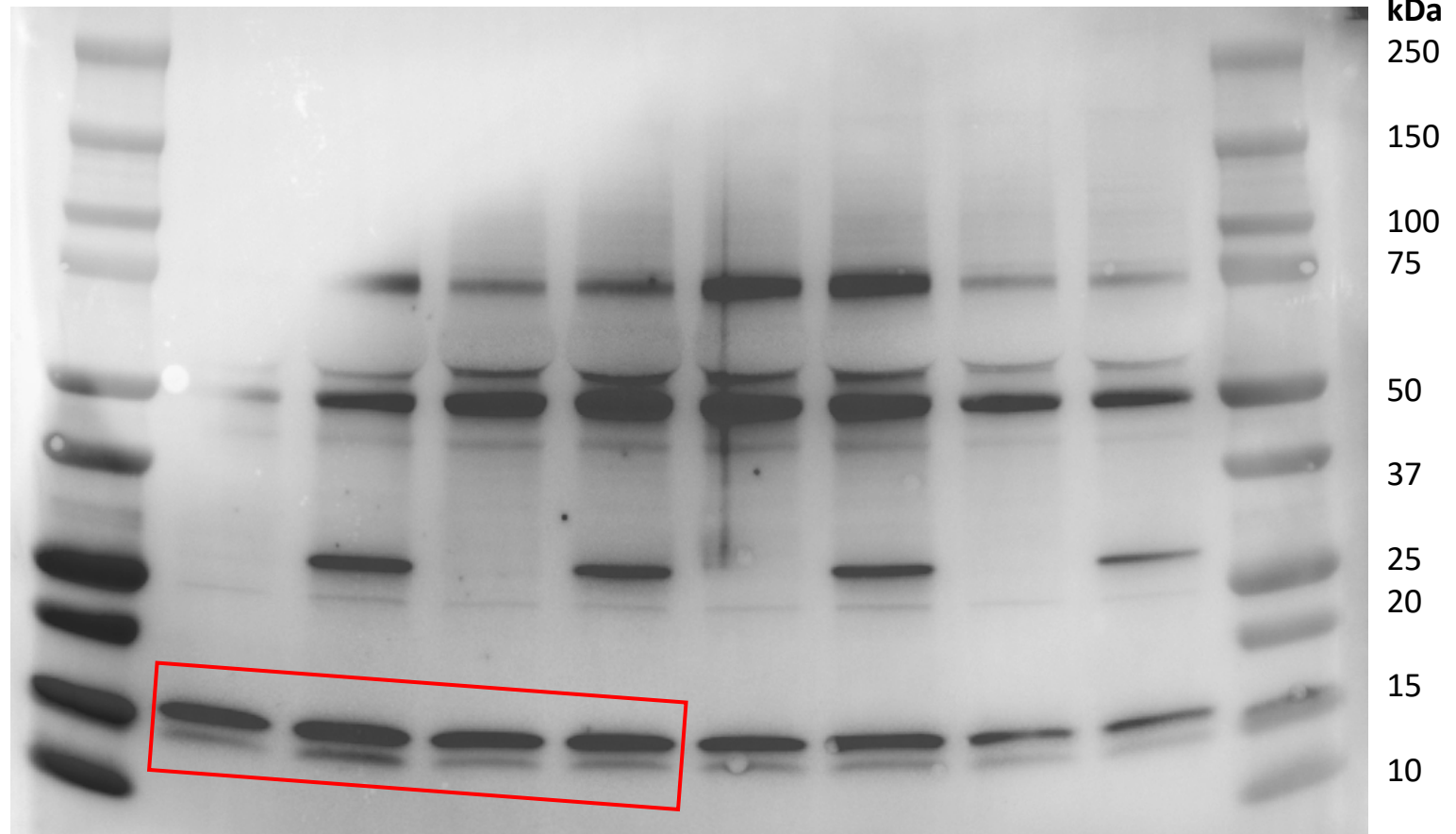


On 4-20% SDS-PAGE stripped after “SQSTM1 after OGD+shBAG3+4-OHT”

LC3 after OGD+shBAG3+4-OHT

Full unedited gel for **Figure.11F**

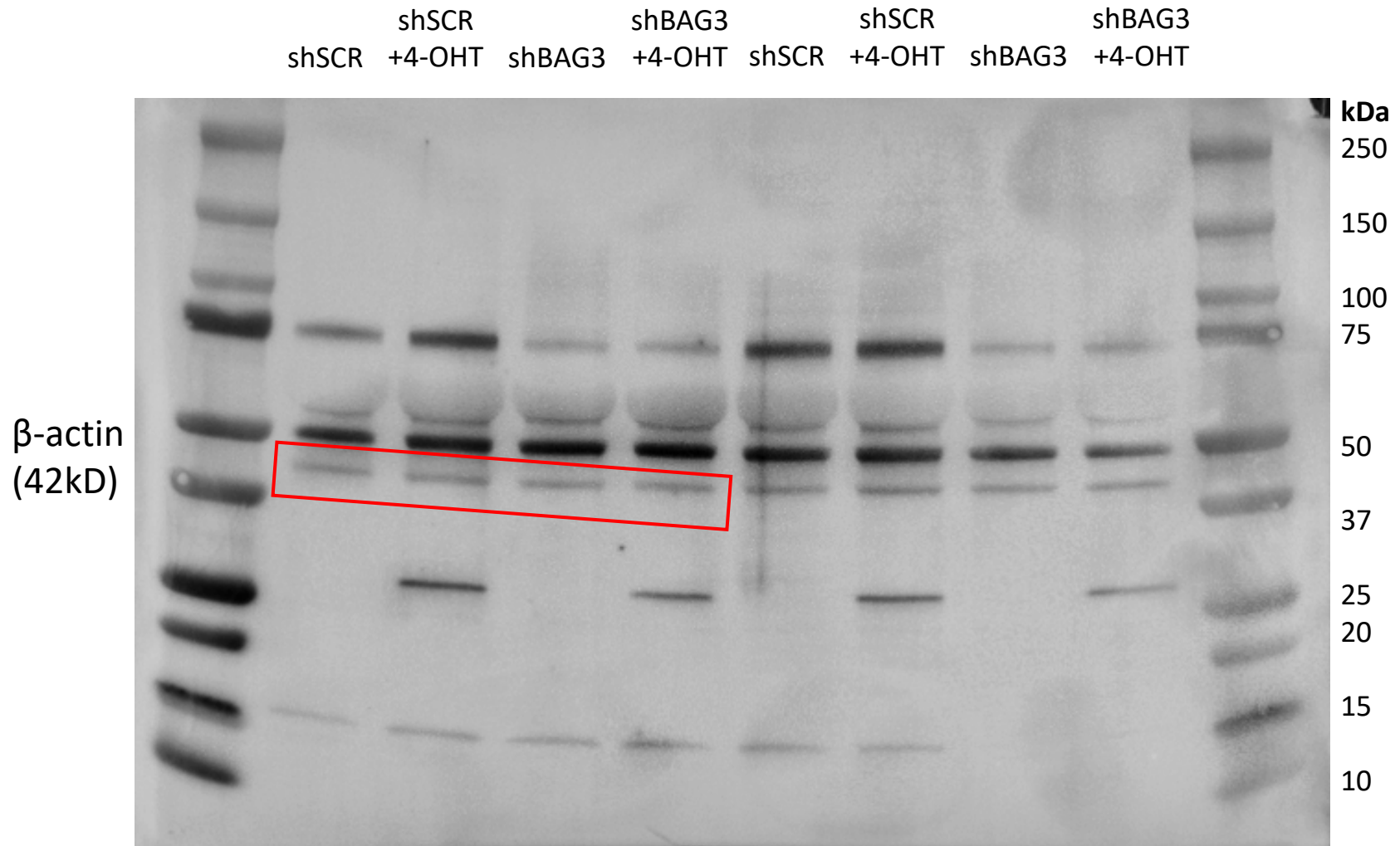
shSCR shBAG3 shSCR shBAG3
shSCR +4-OHT shBAG3 +4-OHT shSCR +4-OHT shBAG3 +4-OHT



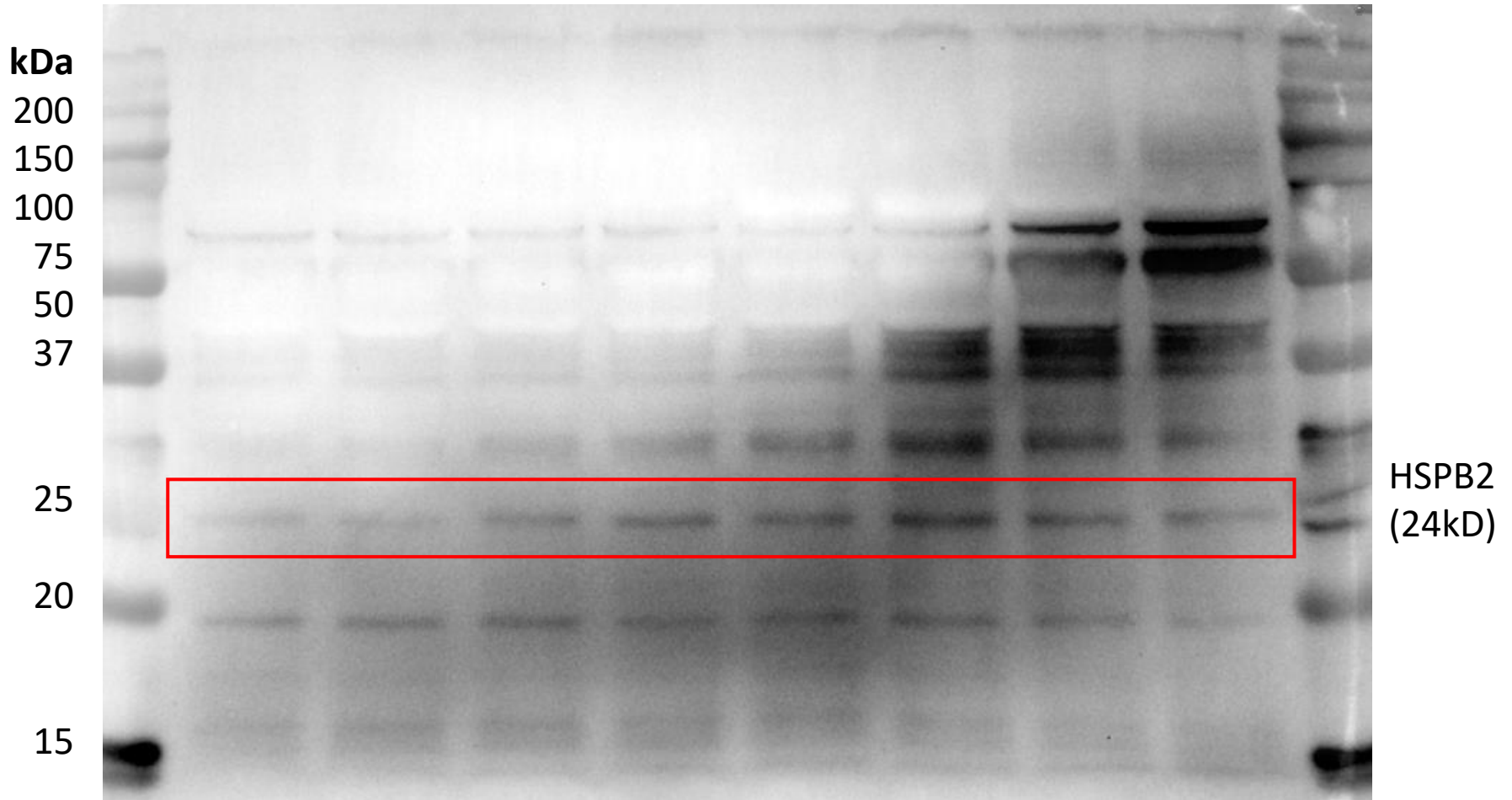
On 4-20% SDS-PAGE stripped after “HSPB2 after OGD+shBAG3+4-OHT”

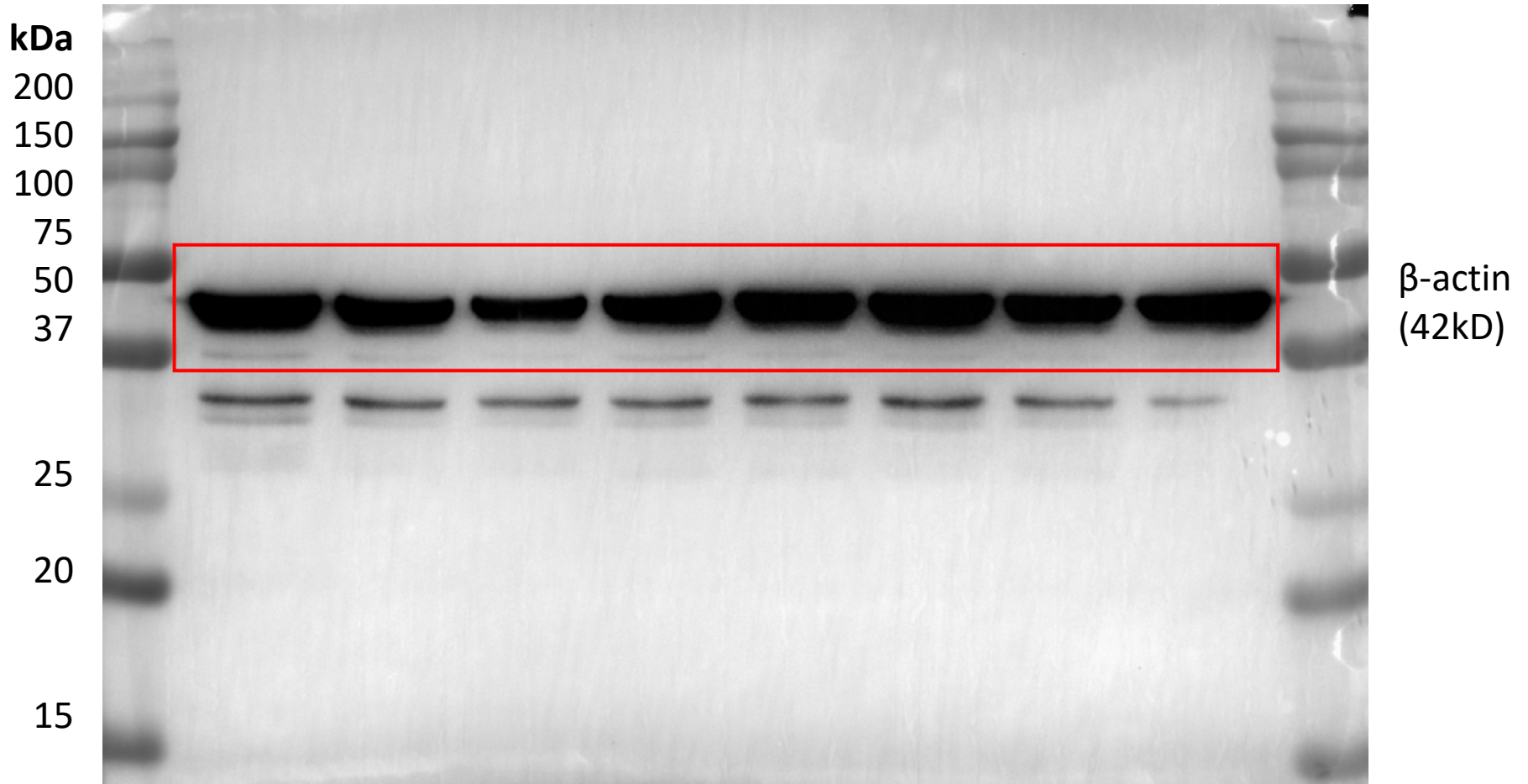
β -actin after OGD+shBAG3+4-OHT

Full unedited gel for **Figure.11F**



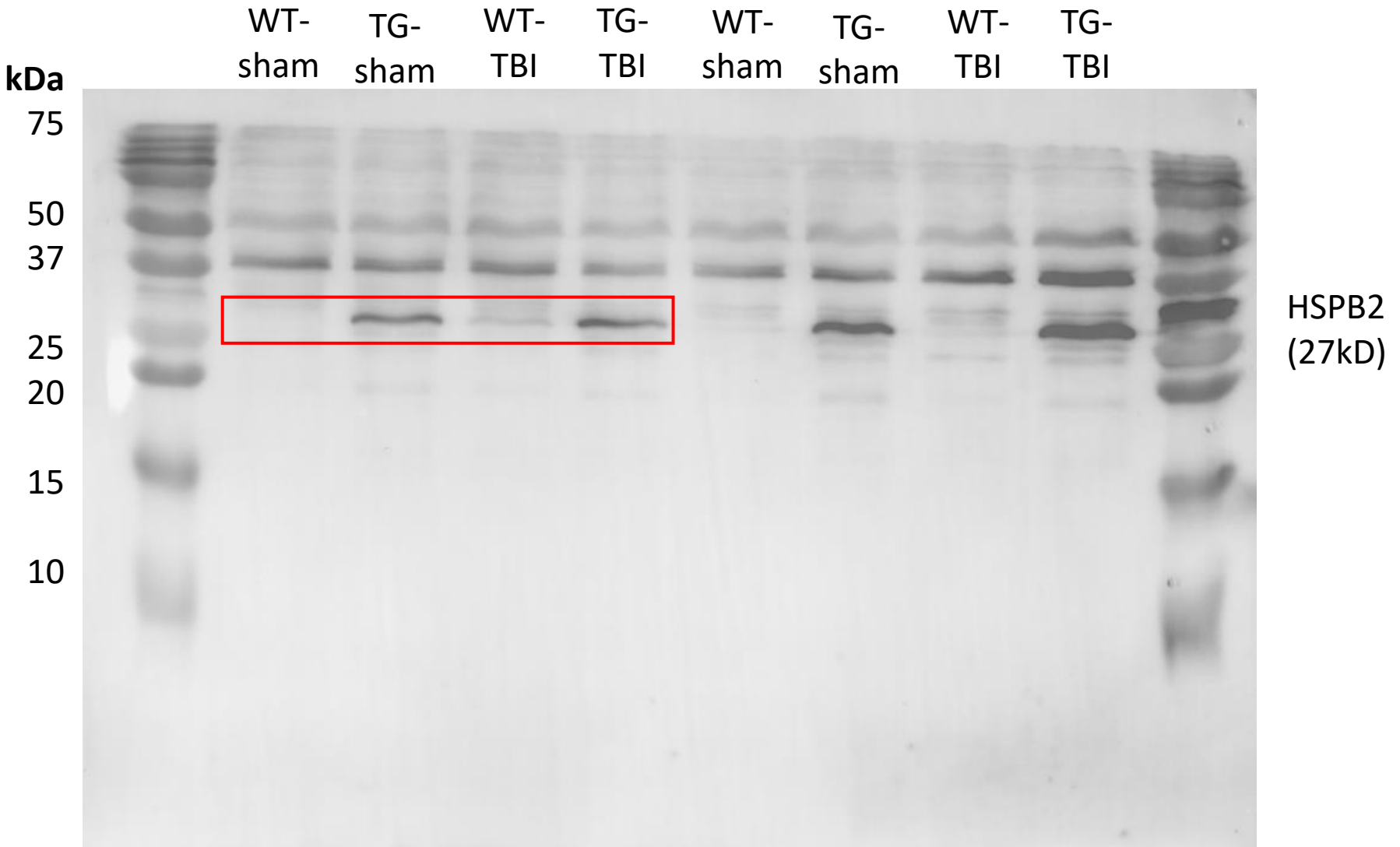
On 4-20% SDS-PAGE stripped after “**LC3 after OGD+shBAG3+4-OHT**”





HSPB2 overexpression

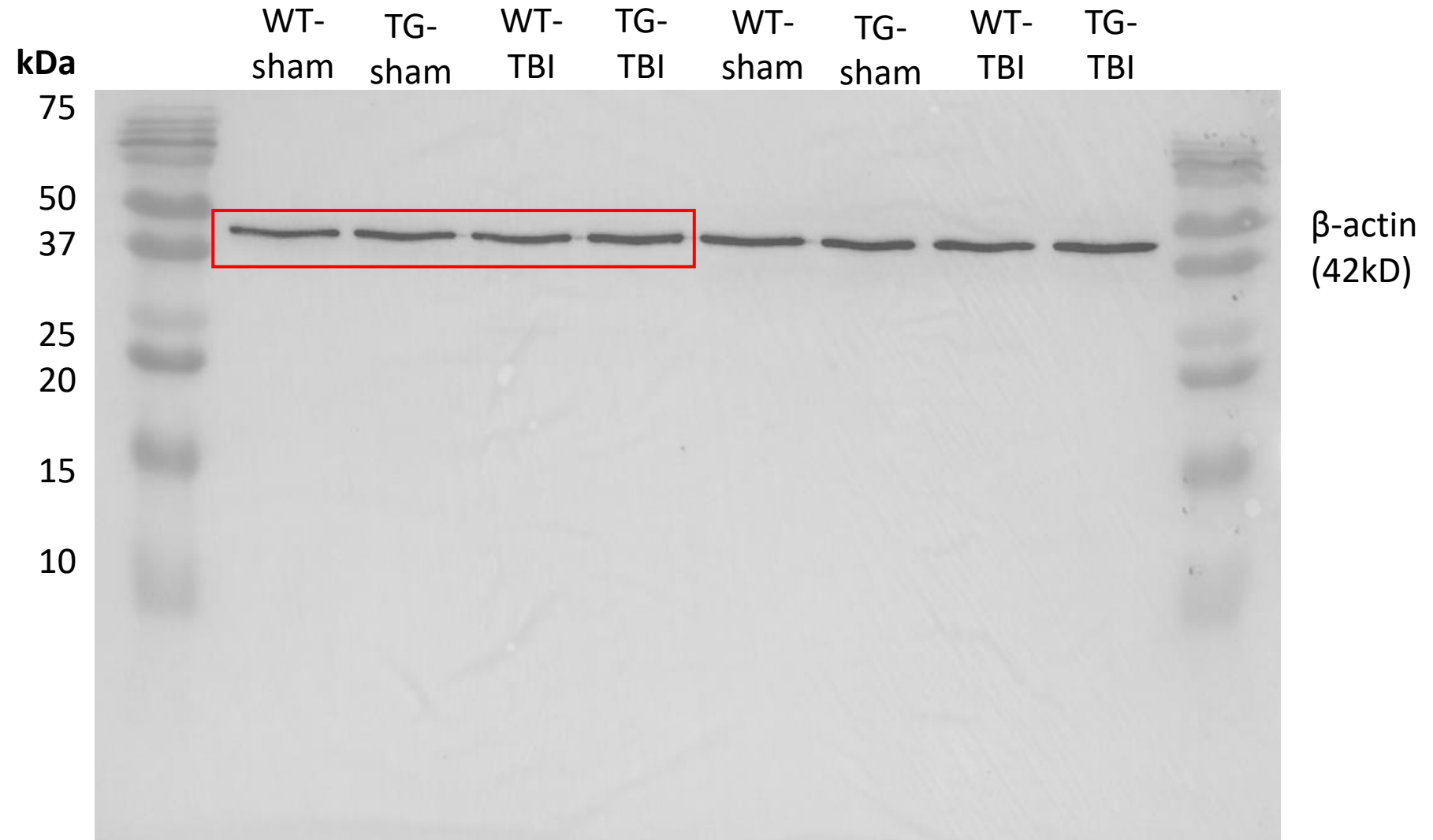
Full unedited gel for **Figure.S2G**



On 15% SDS-PAGE

HSPB2 overexpression

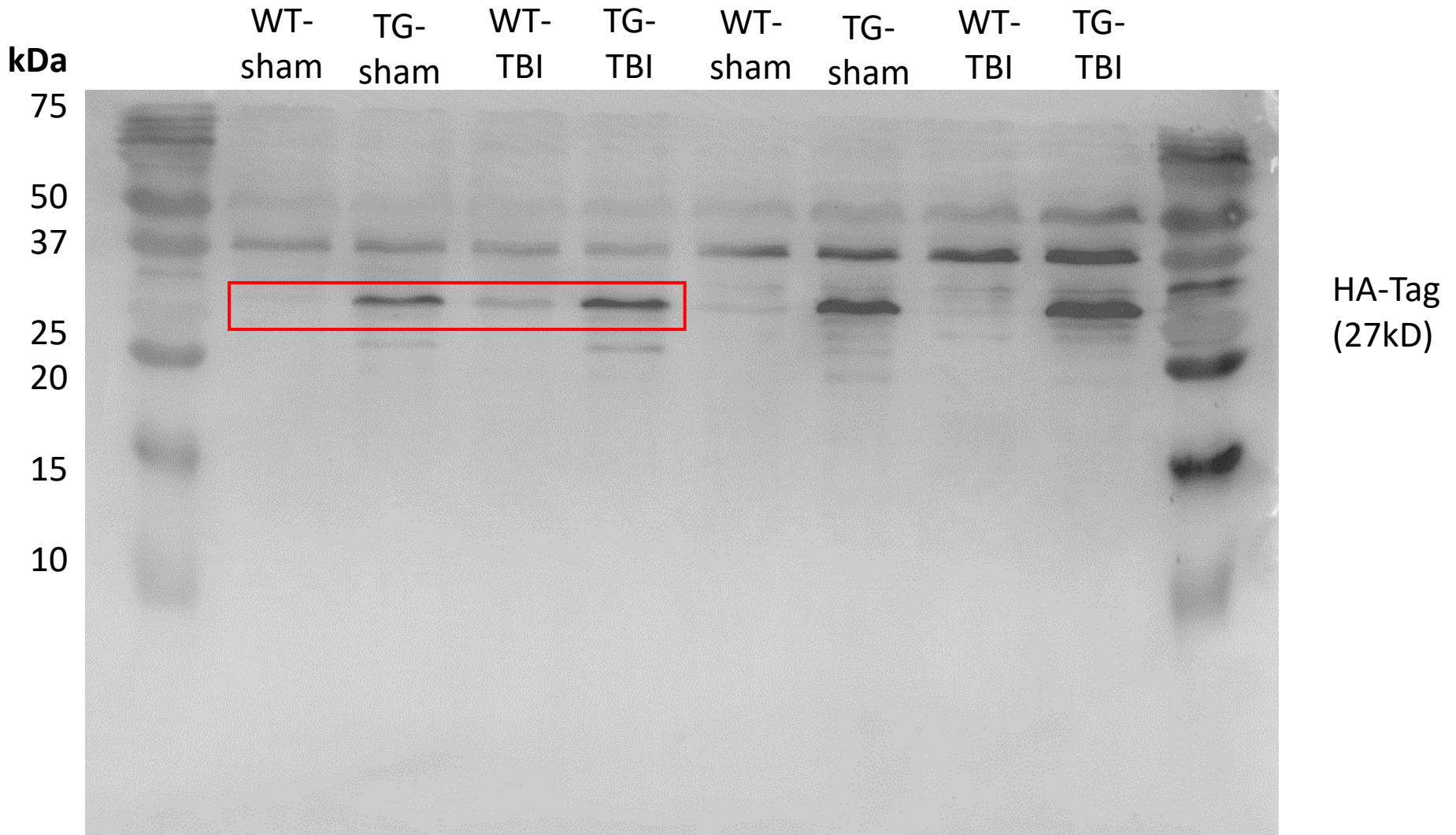
Full unedited gel for **Figure.S2G**



On 15 % SDS-PAGE

HSPB2 overexpression – HA-Tag

Full unedited gel for **Figure.S2G**



On 15 % SDS-PAGE

stripped after “HSPB2 overexpression”